FIG. 6. VAP-B is involved in HCV replication. (A) FLAG–VAP-A (lanes 2 and 5) or FLAG–VAP-B (lanes 3 and 6) was expressed in HEK293T cells and examined by immunoblotting using anti-human VAP-A mouse monoclonal and anti-human VAP-B chicken polyclonal antibodies. (B) In vitro RNA synthesis was carried out in the presence of various concentrations of anti-human VAP-B chicken polyclonal antibody or control chicken IgG. RNA extracted from each fraction was analyzed by agarose gel electrophoresis and autoradiographed. (C) Empty plasmid, expression plasmid of N-terminally HA-tagged VAP-B (HA–VAP-B), or N-terminally HA-tagged VAP-BΔTMD (HA–VAP-BΔTMD) was transfected into HCV replicon cells. Expression of NS5A and NS5B was examined by immunoblotting. (D) HCV RNA was detected by reverse transcription-PCR using primer pairs against NS5A, and expression of G3PDH was used as a control. (E) siRNA against VAP-B or control was transfected into the HCV replicon cells. Lane 1, untreated; lane 2, treated with siFECTOR; lanes 3 and 4, control siRNA was transfected; lanes 5 and 6, VAP-B siRNA was transfected. Expression of NS5A, NS5B, VAP-A, VAP-B, and beta-actin was determined by immunoblotting at 96 h posttransfection. (F) siRNA against VAP-B or control was transfected into the HCV replicon cells. The results are expressed as standard deviations. The significance of the difference in means was determined by the Student t test. The data in each panel are representative of three independent experiments.

NS5A and HCV RNA replication in replicon cells (12). To determine the possible implication of VAP-B in HCV replication, VAP-B or VAP-BΔTMD was expressed in Huh-7 RNA replicon cells. In contrast with the previous data, overexpression of VAP-B increased NS5A and NS5B expression and enhanced the replication of HCV replicon cells, but no effect was observed in cells expressing VAP-BΔTMD (Fig. 6C and D). To confirm the role of VAP-B in HCV replica-

tion, we examined the effect of the knockdown of endogenous VAP-B from the HCV replicon cells by siRNA. At 96 h posttransfection, the expression of VAP-B in cells transfected with the siRNA targeted to VAP-B was reduced to half the levels of cells transfected with a control siRNA, whereas the expression of VAP-A was slightly increased. Although NS5B expression was reduced by the VAP-B knockdown, NS5A was not affected (Fig. 6E). HCV RNA

replication exhibited 25% and 27% reductions by the transfection of 80 and 160 nM siRNA, respectively, to VAP-B (Fig. 6F). Collectively, these results suggest that VAP-B plays an important role in the sequestration of NS5A and NS5B in the HCV RNA replication complex.

DISCUSSION

Although there are conflicting data in the literature, it is accepted that NS5A is a multifunctional protein with critical roles in HCV replication, as well as in the establishment and maintenance of persistent infection (26). Tu et al. were the first to successfully isolate VAP-33 (VAP-A) as a binding partner of NS5A by a yeast two-hybrid screening of the human liver library; they also indicated an association between VAP-A and not only NS5A, but also NS5B, in mammalian cells (48). Gao et al. (12) further demonstrated that NS5A interacts with NS4B, the only HCV NS protein possessing an intrinsic ability to associate with lipid rafts; and the interaction of NS5A, NS5B, NS4B, and other NS proteins with VAP-A on lipid rafts plays a crucial role in the formation of the HCV RNA replication complex (26). Evans et al. indicated that NS5A from the Con1 strain (genotype 1b) is strongly associated with VAP-A, whereas NS5A from the H77 strain (genotype 1a) was unable to bind VAP-A in yeast (9). The determinants of subtype-specific binding to VAP-A were mapped to amino acids 2185 and 2187, and the substitution of these amino acids of the Con1 strain into those of the H77 strain abrogated both the binding to VAP-A and the replication of the subgenomic replicon. However, these defects in binding to VAP-A and in the replication of the subgenomic replicon were suppressed in the highly adaptive S2204I mutation in NS5A. The S2204I adaptive mutation was shown to disrupt NS5A hyperphosphorylation (5), and the loss of NS5A hyperphosphorylation was shown to correlate with the adaptive mutation's ability to suppress the replication defect caused by the VAP-A-noninteracting mutations (9).

To gain more insight into interaction between NS5A and host proteins involved in HCV replication, we screened human libraries by the yeast two-hybrid system using NS5A as bait and identified VAP-B as a binding protein to NS5A. VAP-B is ubiquitously expressed as VAP-A in human tissues, including liver (32). NS5A can bind to both VAP-A and VAP-B and is colocalized in intracellular compartments, such as the ER and Golgi apparatus. The coiled-coil domain of VAP-B is responsible for their interaction with NS5A, as previously reported in VAP-A (48). In the present study, two regions in NS5A are suggested to be important for VAP-B binding. One region is the N-terminal 70 residues, especially from 66 to 70 (2037 to 2042 aa in the HCV polyprotein), although replacement of these 5 residues with Ala could not abrogate binding to VAP-B. The other is identified at the C-terminal polyproline cluster, and replacement of these four residues from 341 to 344 (2313 to 2316 aa in the HCV polyprotein) with Ala in a full-length NS5A reduced VAP-B binding. Two class II polyproline motifs (consensus PXXPXR) are identified in the polyproline cluster and can bind the SH3 domains of a number of cellular signaling proteins, including Grb2 (45), amphiphysin II (56), and Src family tyrosine kinases (25). Pro343 and Leu344 in the C-terminal VAP-B binding region are part of the first class II

polyproline motif. The overlapping of VAP-B's binding region with other cellular signaling proteins may suggest interplay between cellular signaling and replication of HCV. A previous observation indicated that the interaction between NS5A and VAP-A was genotype specific, and amino acid residues critical for the interaction were mapped to amino acids 2185 and 2187 in yeast (9). However, the same authors indicated that NS5A derived from either the 1a or 1b genotype expressed in Huh-7 cells interacted equally well with a glutathione S-transferase fusion VAP-A expressed in bacteria in vitro, and an attempt at selective interaction of hypophosphorylated NS5A from replicon cells with VAP-A was not successful (9). Furthermore, in our study, no clear difference was detected between native NS5A and the S2204I mutant in binding to VAP-A or VAP-B by immunoprecipitation analyses in mammalian cells (data not shown). In addition, the data in Fig. 2 clearly indicate that NS5A genotype 1a binds to both VAP-A and VAP-B, even though this genotype carries the VAP-A-noninteracting mutations (A2185 and G2187). This discrepancy might be explained by the differences between the experimental systems, including the condition of cell lines, the intracellular ratio of VAP-A and VAP-B, and the phosphorylation status of NS5A. Evans et al. proposed that hyperphosphorylated p58 NS5A represents a closed conformation that cannot interact with VAP-A, whereas hypophosphorylated p56 NS5A represents an open conformation capable of strong interaction with VAP-A (9). The phosphorylation of NS5A is a critical modification that controls not only its interaction with VAP-A, but also RNA replication in Huh7 replicon cells (9, 31). Further study will be needed to elucidate the relationship between the phosphorylation status of NS5A and the capability of binding to VAP-B.

The inhibition of HCV RNA replication by the specific antibody to VAP-B in vitro indicated that VAP-B is a component of the HCV RNA replication complex. Furthermore, the reduction of VAP-B expression by siRNA induced the suppression of NS5B expression but not of NS5A, as seen in the knockdown experiment with VAP-A (12). This suggested that VAP plays an important role in the participation of NS5B in the replication complex. VAP could form hetero- and homodimers through their TMDs and interact with NS5A through their coiled-coil domains (Fig. 4). VAP-C is a splicing variant of VAP-B missing 60% of the C terminus. Therefore, VAP-C cannot interact with VAP-A, VAP-B, or NS5A. Although it is difficult to determine precisely the participation of the monomer and dimer of VAP-A and VAP-B in the HCV replication complex, it might be plausible to speculate that VAP-A is expressed more abundantly than VAP-B and that the heterodimer of VAP-A and VAP-B is more active as an HCV replication complex than those of the monomeric or homodimeric forms. Therefore, overexpression of VAP-B, but not of VAP-A, enhanced HCV RNA replication by providing scaffolds in appropriate positions, like the raft-like domain in the ER/Golgi compartment, capable of changing the nonfunctional NS proteins into a replication-competent state, because only a small fraction of NS proteins are functional as replication complexes (20, 28). Furthermore, VAP-A might have a higher affinity to NS5B than VAP-B does, and overexpression of the TMD deletion mutant of VAP-A, but not that of VAP-B, exhibited a reduction of RNA replication (12). The

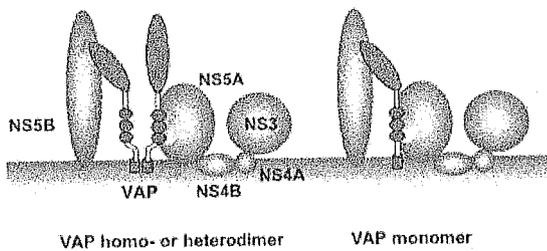VAP homo- or heterodimer   VAP monomer

FIG. 7. Models of interaction between HCV NS proteins and VAP. Monomeric and hetero- or homodimeric forms of VAPs can interact with NS5A and NS5B through the coiled-coil domain and N-terminal region, respectively. NS4B can associate with lipid rafts and interact with NS5A (9). NS4A is a cofactor of NS3 and recruits NS3 to the HCV NS protein complex.

possible implication of monomeric and dimeric forms of VAPs in the replication complex of HCV is shown in Fig. 7.

In this study, we identified VAP-B as a novel binding protein to NS5A and NS5B and demonstrated its participation in HCV RNA replication. Elucidation of the precise roles of VAP-A and VAP-B in the phosphorylation of NS5A and in the formation of the replication complex through interaction with other HCV NS proteins and host proteins should provide clues to understanding the molecular mechanisms underlying the replication of HCV RNA and to developing novel therapeutics for chronic hepatitis C.

ACKNOWLEDGMENTS

REFERENCES

1. Aizaki, H., Y. Aoki, T. Harada, K. Ishii, T. Suzuki, S. Nagamori, G. Toda, Y. Matsuura, and T. Miyamura. 1998. Full-length complementary DNA of hepatitis C virus genome from an infectious blood sample. Hepatology 27: 621–627.
2. Aizaki, H., K. Lee, V. M.-H. Sung, H. Ishiki, and M. M. C. Lai. 2004. Characterization of the hepatitis C virus RNA replication complex associated with lipid rafts. Virology 324:450–461.
3. Ali, N., K. D. Tardif, and A. Siddiqui. 2002. Cell-free replication of the hepatitis C virus subgenomic replicon. J. Virol. 76:12001–12007.
4. Appel, N., T. Pietschmann, and R. Bartenschlager. 2005. Mutational analysis of hepatitis C virus nonstructural protein 5A: potential role of differential phosphorylation in RNA replication and identification of a genetically flexible domain. J. Virol. 79:3187–3194.
5. Blight, K. J., J. A. McKeating, J. Marcotrigiano, and C. M. Rice. 2003. Efficient replication of hepatitis C virus genotype 1a RNAs in cell culture. J. Virol. 77:3181–3190.
6. Cerny, A., and F. V. Chisari. 1999. Pathogenesis of chronic hepatitis C: immunological features of hepatic injury and viral persistence. Hepatology 30:595–601.
7. Christopher, V., N. Scolding, and R. T. Przemioslo. 2005. Acute hepatitis secondary to interferon beta-1a in multiple sclerosis. J. Neurol. 252:855–856.
8. Chung, K. M., J. Lee, J. E. Kim, O. K. Song, S. Cho, J. Lim, M. Seedorf, B. Hahm, and S. K. Jang. 2000. Nonstructural protein 5A of hepatitis C virus inhibits the function of karyopherin β3. J. Virol. 74:5233–5241.
9. Evans, M. J., C. M. Rice, and S. P. Goff. 2004. Phosphorylation of hepatitis C virus nonstructural protein 5A modulates its protein interactions and viral RNA replication. Proc. Natl. Acad. Sci. USA 101:13038–13043.
10. Foster, L. J., M. L. Weir, D. Y. Lim, Z. Liu, W. S. Trimble, and A. Klip. 2000.

A functional role for VAP-33 in insulin-stimulated GLUT4 traffic. Traffic 1:512–521.
11. Gale, M. J., Jr., M. J. Korth, N. M. Tang, S. L. Tan, D. A. Hopkins, T. E. Dever, S. J. Polyak, D. R. Gretch, and M. G. Katze. 1997. Evidence that hepatitis C virus resistance to interferon is mediated through repression of the PKR protein kinase by the nonstructural 5A protein. Virology 230:217–227.
12. Gao, L., H. Aizaki, J. W. He, and M. M. Lai. 2004. Interactions between viral nonstructural proteins and host protein hVAP-33 mediate the formation of hepatitis C virus RNA replication complex on lipid raft. J. Virol. 78:3480–3488.
13. Girod, A., B. Storrie, J. C. Simpson, L. Johannes, B. Goud, L. M. Roberts, J. M. Lord, T. Nilsson, and R. Pepperkok. 1999. Evidence for a COP-I-independent transport route from the Golgi complex to the endoplasmic reticulum. Nat. Cell Biol. 1:423–430.
14. Hardy, R. W., J. Marcotrigiano, K. J. Blight, J. E. Majors, and C. M. Rice. 2003. Hepatitis C virus RNA synthesis in a cell-free system isolated from replicon-containing hepatoma cells. J. Virol. 77:2029–2037.
15. He, Y., H. Nakao, S. L. Tan, S. J. Polyak, P. Neddermann, S. Vijaysri, B. L. Jacobs, and M. G. Katze. 2002. Subversion of cell signaling pathways by hepatitis C virus nonstructural 5A protein via interaction with Grb2 and P85 phosphatidylinositol 3-kinase. J. Virol. 76:9207–9217.
16. Ho, S. N., H. D. Hunt, R. M. Horton, J. K. Pullen, and L. R. Pease. 1989. Site-directed mutagenesis by overlap extension using the polymerase chain reaction. Gene 77:51–59.
17. Horton, R. M., H. D. Hunt, S. N. Ho, J. K. Pullen, and L. R. Pease. 1989. Engineering hybrid genes without the use of restriction enzymes: gene splicing by overlap extension. Gene 77:61–68.
18. Huang, D. C., S. Cory, and A. Strasser. 1997. Bcl-2, Bcl-XL and adenovirus protein E1B19kD are functionally equivalent in their ability to inhibit cell death. Oncogene 14:405–414.
19. Kapadia, S. B., and F. V. Chisari. 2005. Hepatitis C virus RNA replication is regulated by host geranylgeranylation and fatty acids. Proc. Natl. Acad. Sci. USA 102:2561–2566.
20. Kishine, H., K. Sugiyama, M. Hijikata, N. Kato, H. Takahashi, T. Noshi, Y. Nio, M. Hosaka, Y. Miyanari, and K. Shimotohno. 2002. Subgenomic replicon derived from a cell line infected with the hepatitis C virus. Biochem. Biophys. Res. Commun. 293:993–999.
21. Koch, J. O., and R. Bartenschlager. 1999. Modulation of hepatitis C virus NS5A hyperphosphorylation by nonstructural proteins NS3, NS4A, and NS4B. J. Virol. 73:7138–7146.
22. Lapierre, L. A., P. L. Tuma, J. Navarre, J. R. Goldenring, and J. M. Anderson. 1999. VAP-33 localizes to both an intracellular vesicle population and with occludin at the tight junction. J. Cell Sci. 112:3723–3732.
23. Loewen, C. J., and T. P. Levine. 2005. A highly conserved binding site in VAP for the FFAT motif of lipid binding proteins. J. Biol. Chem. 280:14097–14104.
24. Lohmann, V., F. Korner, J. Koch, U. Herian, L. Theilmann, and R. Bartenschlager. 1999. Replication of subgenomic hepatitis C virus RNAs in a hepatoma cell line. Science 285:110–113.
25. Macdonald, A., K. Crowder, A. Street, C. McCormick, and M. Harris. 2004. The hepatitis C virus NS5A protein binds to members of the Src family of tyrosine kinases and regulates kinase activity. J. Gen. Virol. 85:721–729.
26. Macdonald, A., and M. Harris. 2004. Hepatitis C virus NS5A: tales of a promiscuous protein. J. Gen. Virol. 85:2485–2502.
27. Majumder, M., A. K. Ghosh, R. Steele, R. Ray, and R. B. Ray. 2001. Hepatitis C virus NS5A physically associates with p53 and regulates p21/waf1 gene expression in a p53-dependent manner. J. Virol. 75:1401–1407.
28. Miyanari, Y., M. Hijikata, M. Yamaji, M. Hosaka, H. Takahashi, and K. Shimotohno. 2003. Hepatitis C virus non-structural proteins in the probable membranous compartment function in viral genome replication. J. Biol. Chem. 278:50301–50308.
29. Moriishi, K., and Y. Matsuura. 2003. Mechanisms of hepatitis C virus infection. Antivir. Chem. Chemother. 14:285–297.
30. Neddermann, P., A. Clementi, and R. De Francesco. 1999. Hyperphosphorylation of the hepatitis C virus NS5A protein requires an active NS3 protease, NS4A, NS4B, and NS5A encoded on the same polyprotein. J. Virol. 73:9984–9991.
31. Neddermann, P., M. Quintavalle, C. Di Pietro, A. Clementi, M. Cerretani, S. Altamura, L. Bartholomew, and R. De Francesco. 2004. Reduction of hepatitis C virus NS5A hyperphosphorylation by selective inhibition of cellular kinases activates viral RNA replication in cell culture. J. Virol. 78:13306–13314.
32. Nishimura, Y., M. Hayashi, H. Inada, and T. Tanaka. 1999. Molecular cloning and characterization of mammalian homologues of vesicle-associated membrane protein-associated (VAMP-associated) proteins. Biochem. Biophys. Res. Commun. 254:21–26.
33. Niwa, H., K. Yamamura, and J. Miyazaki. 1991. Efficient selection for high-expression transfectants with a novel eukaryotic vector. Gene 108:193–199.
34. O'Connor, L., A. Strasser, L. A. O'Reilly, G. Hausmann, J. M. Adams, S.

Cory, and D. C. Huang. 1998. Bim: a novel member of the Bcl-2 family that promotes apoptosis. EMBO J. 17:384–395.

35. Pawlotsky, J. M., and G. Germanidis. 1999. The non-structural 5A protein of hepatitis C virus. J. Viral. Hepat. 6:343–356.

36. Pietschmann, T., V. Lohmann, G. Rutter, K. Kurpanek, and R. Bartenschlager. 2001. Characterization of cell lines carrying self-replicating hepatitis C virus RNAs. J. Virol. 75:1252–1264.

37. Qadri, I., M. Iwahashi, and F. Simon. 2002. Hepatitis C virus NS5A protein binds TBP and p53, inhibiting their DNA binding and p53 interactions with TBP and ERCC3. Biochim. Biophys. Acta 1592:193–204.

38. Schoch, S., F. Deak, A. Konigstorfer, M. Mozhayeva, Y. Sara, T. C. Sudhof, and E. T. Kavalali. 2001. SNARE function analyzed in synaptobrevin/VAMP knockout mice. Science 294:1117–1122.

39. Shi, S. T., K. J. Lee, H. Aizaki, S. B. Hwang, and M. M. Lai. 2003. Hepatitis C virus RNA replication occurs on a detergent-resistant membrane that cofractionates with caveolin-2. J. Virol. 77:4160–4168.

40. Shi, S. T., S. J. Polyak, H. Tu, D. R. Taylor, D. R. Gretch, and M. M. Lai. 2002. Hepatitis C virus NS5A colocalizes with the core protein on lipid droplets and interacts with apolipoproteins. Virology 292:198–210.

41. Shimakami, T., M. Hijikata, H. Luo, Y. Y. Ma, S. Kaneko, K. Shimotohno, and S. Murakami. 2004. Effect of interaction between hepatitis C virus NS5A and NS5B on hepatitis C virus RNA replication with the hepatitis C virus replicon. J. Virol. 78:2738–2748.

42. Skehel, P. A., R. Fabian-Fine, and E. R. Kandel. 2000. Mouse VAP33 is associated with the endoplasmic reticulum and microtubules. Proc. Natl. Acad. Sci. USA 97:1101–1106.

43. Skehel, P. A., K. C. Martin, E. R. Kandel, and D. Bartsch. 1995. A VAMP-binding protein from Aplysia required for neurotransmitter release. Science 269:1580–1583.

44. Soussan, L., D. Burakov, M. P. Daniels, M. Toister-Achituv, A. Porat, Y. Yarden, and Z. Elazar. 1999. ERG30, a VAP-33-related protein, functions in protein transport mediated by COPI vesicles. J. Cell Biol. 146:301–311.

45. Tan, S. L., H. Nakao, Y. He, S. Vijaysri, P. Neddermann, B. L. Jacobs, B. J. Mayer, and M. G. Katze. 1999. NS5A, a nonstructural protein of hepatitis C virus, binds growth factor receptor-bound protein 2 adaptor protein in a Src homology 3 domain/ligand-dependent manner and perturbs mitogenic signaling. Proc. Natl. Acad. Sci. USA 96:5533–5538.

46. Tellinghuisen, T. L., J. Marcotrigiano, A. E. Gorbalenya, and C. M. Rice. 2004. The NS5A protein of hepatitis C virus is a zinc metalloprotein. J. Biol. Chem. 279:48576–48587.

47. Tellinghuisen, T. L., J. Marcotrigiano, and C. M. Rice. 2005. Structure of the zinc-binding domain of an essential component of the hepatitis C virus replicase. Nature 435:374–379.

48. Tu, H., L. Gao, S. T. Shi, D. R. Taylor, T. Yang, A. K. Mircheff, Y. Wen, A. E. Gorbalenya, S. B. Hwang, and M. M. Lai. 1999. Hepatitis C virus RNA polymerase and NS5A complex with a SNARE-like protein. Virology 263:30–41.

49. Wang, C., M. Gale, Jr., B. C. Keller, H. Huang, M. S. Brown, J. L. Goldstein, and J. Ye. 2005. Identification of FBL2 as a geranylgeranylated cellular protein required for hepatitis C virus RNA replication. Mol. Cell 18:425–434.

50. Weir, M. L., A. Klip, and W. S. Trimble. 1998. Identification of a human homologue of the vesicle-associated membrane protein (VAMP)-associated protein of 33 kDa (VAP-33): a broadly expressed protein that binds to VAMP. Biochem. J. 333:247–251.

51. Weir, M. L., H. Xie, A. Klip, and W. S. Trimble. 2001. VAP-A binds promiscuously to both v- and tSNAREs. Biochem. Biophys. Res. Commun. 286:616–621.

52. Yanagi, M., R. H. Purcell, S. U. Emerson, and J. Bukh. 1997. Transcripts from a single full-length cDNA clone of hepatitis C virus are infectious when directly transfected into the liver of a chimpanzee. Proc. Natl. Acad. Sci. USA 94:8738–8743.

53. Yang, G., D. C. Pevear, M. S. Collett, S. Chunduru, D. C. Young, C. Benetatos, and R. Jordan. 2004. Newly synthesized hepatitis C virus replicon RNA is protected from nuclease activity by a protease-sensitive factor(s). J. Virol. 78:10202–10205.

54. Ye, J., C. Wang, R. Sumpter, Jr., M. S. Brown, J. L. Goldstein, and M. Gale, Jr. 2003. Disruption of hepatitis C virus RNA replication through inhibition of host protein geranylgeranylation. Proc. Natl. Acad. Sci. USA 100:15865–15870.

55. Yi, M., and S. M. Lemon. 2004. Adaptive mutations producing efficient replication of genotype 1a hepatitis C virus RNA in normal Huh7 cells. J. Virol. 78:7904–7915.

56. Zech, B., A. Kurtenbach, N. Krieger, D. Strand, S. Blencke, M. Morbitzer, K. Salassidis, M. Cotten, J. Wissing, S. Obert, R. Bartenschlager, T. Herget, and H. Daub. 2003. Identification and characterization of amphiphysin II as a novel cellular interaction partner of the hepatitis C virus NS5A protein. J. Gen. Virol. 84:555–560.

Essential Elements of the Capsid Protein for Self-Assembly into Empty Virus-Like Particles of Hepatitis E Virus

Tian-Cheng Li,[1]* Naokazu Takeda,[1] Tatsuo Miyamura,[1] Yoshiharu Matsuura,[2] Joseph C. Y. Wang,[3] Helena Engvall,[3] Lena Hammar,[3] Li Xing,[3] and R. Holland Cheng[3,4]

Department of Virology II, National Institute of Infectious Diseases, Gakuen 4-7-1, Musashi-Murayama, Tokyo 208-0011,[1] and Department of Molecular Virology, Research Institute for Microbial Diseases, Osaka University, Suita-shi, Osaka 565-0871,[2] Japan; Karolinska Institute, Department of Biosciences, 141 57 Huddinge, Sweden[3]; and Department of Molecular and Cellular Biology, University of California, Davis, California 95616[4]

Hepatitis E virus (HEV) is a noncultivable virus that causes acute liver failure in humans. The virus's major capsid protein is encoded by an open reading frame 2 (ORF2) gene. When the recombinant protein consisting of amino acid (aa) residues 112 to 660 of ORF2 is expressed with a recombinant baculovirus, the protein self-assembles into virus-like particles (VLPs) (T.-C. Li, Y. Yamakawa, K. Suzuki, M. Tatsumi, M. A. Razak, T. Uchida, N. Takeda, and T. Miyamura, J. Virol. 71:7207–7213, 1997). VLPs can be found in the culture medium of infected Tn5 cells but not in that of Sf9 cells, and the major VLPs have lost the C-terminal 52 aa. To investigate the protein requirement for HEV VLP formation, we prepared 14 baculovirus recombinants to express the capsid proteins truncated at the N terminus, the C terminus, or both. The capsid protein consisting of aa residues 112 to 608 formed VLPs in Sf9 cells, suggesting that particle formation is dependent on the modification process of the ORF2 protein. In the present study, electron cryomicroscopy and image processing of VLPs produced in Sf9 and Tn5 cells indicated that they possess the same configurations and structures. Empty VLPs were found in both Tn5 and Sf9 cells infected with the recombinant containing an N-terminal truncation up to aa residue 125 and C-terminal to aa residue 601, demonstrating that the aa residues 126 to 601 are the essential elements required for the initiation of VLP assembly. The recombinant HEV VLPs are potential mucosal vaccine carrier vehicles for the presentation of foreign antigenic epitopes and may also serve as vectors for the delivery of genes to mucosal tissue for DNA vaccination and gene therapy. The results of the present study provide useful information for constructing recombinant HEV VLPs having novel functions.

Hepatitis E virus (HEV), which causes severe acute liver failure, belongs to the genus *Hepevirus* in the family *Hepeviridae* (22). HEV contains an approximately 7.2-kb single-stranded positive-sense RNA molecule (21). The RNA is 3' polyadenylated and includes three open reading frames (ORF). ORF1, mapped in the 5' half of the genome, encodes viral nonstructural proteins (7, 12). ORF2, located at the 3' terminus of the genome, encodes a protein-forming viral capsid (11, 25). ORF3, mapped between ORF1 and ORF2, encodes a 13.5-kDa protein that is associated with the membrane as well as with the cytoskeleton fraction (27). This protein is shown to be phosphorylated by the cellular mitogen-activated protein kinase (6, 8). The ORF3 protein may have a regulatory function (6, 8). Ever since HEV was first discovered in 1980 and visualized by immune electron microscopy in 1983 (2), many efforts have been made, using different expression systems, to express the structural protein (5, 11, 17, 26). It is particularly important to characterize the viral protein because so far no practical cell culture system for growing HEV is available. Only one neutralization epitope has been identified; it maps between amino acids 578 and 607 of the ORF2 protein (pORF2) (18).

The expression of foreign proteins in baculovirus systems opens the prospect of studying HEV capsid assembly, since virus-like particles (VLPs) of pronounced spikes on the surface can be formed with the recombinant protein expressed with this system (11, 25). This VLP is capable of inducing systemic and mucosal immune responses in experimental animals (9). With an oral inoculation of 10 mg of recombinant HEV VLPs, cynomolgus monkeys can develop anti-HEV immunoglobulin M (IgM), IgG, and IgA responses and protect against HEV infection (10). All these data suggest that VLPs are a candidate HEV vaccine.

The VLPs produced from Tn5 cells appear as T=1 icosahedral particles, which are composed of 60 copies of truncated pORF2 (25). The protein contains two distinctive domains: the shell (S) domain forms the semiclosed icosahedral shell, while the protrusion (P) domain interacts with the neighboring proteins to form the protrusion. The projection of T=1 recombinant HEV VLPs appears as spikes decorated with spherical rings (25), which fits with the morphology obtained from negatively stained HEV native virions. The diameter of these VLPs, 27 nm, is less than that reported for partially purified native virions (16). However, VLPs retain the antigenicity of the native HEV virion by designated antigenic sites at the P domain and by the capsid connection at the S domain. The particles appear empty, with no significant RNA-like density inside. The N-terminal region of pORF2 is rich in positively charged amino acid residues and may interact with RNA mol-

---

* Corresponding author. Mailing address: Department of Virology II, National Institute of Infectious Diseases, Gakuen 4-7-1, Musashi-Murayama, Tokyo 208-0011, Japan. Phone: (81)-42-561-0771. Fax: (81)-42-561-4729. E-mail: litc@nih.go.jp.

TABLE 1. Oligonucleotides used in the construction of baculovirus recombinants

Recombinant baculovirus	Forward primer[a]	Reverse primer[b]
Ac[n111]	AAGGATCCATGGCGGTCGCTCCAGCCCATGACACCCCGCCAGT	GGTCTAGACTATAACTCCCGAGTTTTACCCACCTTCTACTT
Ac[n111c52]	AAGGATCCATGGCGGTCGCTCCAGCCCATGACACCCCGCCAGT	AATCTAGACTATGCTAGCGCAGAGTGGGGGGCTAAAA
Ac[n111c58]	AAGGATCCATGGCGGTCGCTCCAGCCCATGACACCCCGCCAGT	AATCTAGACTAGGCTAAAACAGCAACCGCAGAGATGG
Ac[n111c59]	AAGGATCCATGGCGGTCGCTCCAGCCCATGACACCCCGCCAGT	AATCTAGACTATAAAACAGCAACCGCAGAGATGGAGA
Ac[n111c60]	AAGGATCCATGGCGGTCGCTCCAGCCCATGACACCCCGCCAGT	AATCTAGACTAAACAGCAACCGCAGAGATGGAGACGG
Ac[n111c64]	AAGGATCCATGGCGGTCGCTCCAGCCCATGACACCCCGCCAGT	AATCTAGACTAAGAGATGGAGACGGGACCAGCACCCA
Ac[n111c72]	AAGGATCCATGGCGGTCGCTCCAGCCCATGACACCCCGCCAGT	AATCTAGACTAACCCAGGCTAGTGGTGTAAGTGGAAA
Ac[c52]	CAGGATCCATGCGCCCTCGGCCTATTTTGTTGCTGCT	AATCTAGACTATGCTAGCGCAGAGTGGGGGGCTAAAA
Ac[n123]	AAGGATCCATGGATGTCGACTCTCGCGGCGCCATCTT	GGTCTAGACTATAACTCCCGAGTTTTACCCACCTTCTACTT
Ac[n124]	AAGGATCCATGGTCGACTCTCGCGGCGCCATCTT	GGTCTAGACTATAACTCCCGAGTTTTACCCACCTTCTACTT
Ac[n125]	AAGGATCCATGGACTCTCGCGGCGCCATCTTGCG	GGTCTAGACTATAACTCCCGAGTTTTACCCACCTTCTACTT
Ac[n126]	AAGGATCCATGTCTCGCGGCGCCATCTTGCGCCG	GGTCTAGACTATAACTCCCGAGTTTTACCCACCTTCTACTT
Ac[n130]	CAGGATCCATGATCTTGCGCCGGCAGTATAATCTATC	GGTCTAGACTATAACTCCCGAGTTTTACCCACCTTCTACTT
Ac[n125c59]	AAGGATCCATGGACTCTCGCGGCGCCATCTTGCG	AATCTAGACTATAAAACAGCAACCGCAGAGATGGAGA

[a] BamHI (underlined) and an initiation codon (bold) are indicated.
[b] XbaI (underlined) and a stop codon (bold) are indicated.

ecules (21). Thus, the deletion of the N-terminal 111 amino acid (aa) residues and the insufficient volume of the central cavity may lead to the failure of RNA encapsidation (25).

Cell type dependence in the VLP formation of the recombinant capsid protein was observed when aa residues 112 to 660 of ORF2 were expressed with a recombinant baculovirus in two insect cell lines, Tn5 and Sf9. In Tn5 cells, two major bands, having molecular masses of 58 kDa (58K) and 53 kDa (53K), were found in the cell lysate, while a peptide in the VLPs comprising a 53K protein was found in the culture medium. The 53K protein has been designated as either the 50K or 54K protein in previous studies (9, 11). In Sf9 cells, an additional peptide with a size between that of 58K and that of 53K was found in the cell lysate. However, no VLP was recovered from the culture medium. In Tn5 cells, terminal sequencing revealed that 58K and 53K proteins have the same first 15 aa in the N terminus and that a posttranslation cleavage by cellular protease(s) occurred at the pORF2 C termini and converted 58K into 53K. An independent but similar observation was obtained when pORF2 of the Pakistani strain was expressed in Sf9 cells (17) where several immunoactive proteins were detected in the cell lysate, and a 53K protein was secreted into the culture medium, but no VLP was found. Further investigation of pORF2 expression in Sf9 and Tn5 cells may allow us to understand the mechanism underlying the subunit assembly and particle formation of the recombinant HEV capsid.

We analyzed particle formation with pORF2 containing a series of truncated deletions at the N- and/or C-terminal region. In both Sf9 and Tn5 cells, amino acid residues 126 to 601 appeared to form the pORF2 core structure and were capable of self-assembling into VLPs. These results indicated that the cell dependence on particle formation is due to the difference between Sf9 and Tn5 cells in the modification process of pORF2.

MATERIALS AND METHODS

Generation of recombinant baculoviruses and expression of capsid proteins. DNA fragments encoding the N- and/or C-terminal aa-truncated pORF2 were amplified by PCR using plasmid pHEV5134/7161 as a template. Plasmid pHEV5134/7161 containing a full-length genotype I (G1) HEV pORF2 was

described previously (11). The primers used in the construction of baculovirus recombinants are shown in Table 1. Amplified DNA fragments were purified by using a QIAGEN PCR purification kit (QIAGEN, Valencia, CA), digested with restriction enzymes, and ligated with baculovirus transfer vector pVL1393 (Pharmingen, San Diego, CA). An insect cell line derived from *Spodoptera frugiperda* (Sf9) (19) (Riken Cell Bank, Tsukuba, Japan) was cotransfected with a linearized wild-type *Autographa californica* nuclear polyhedrosis virus DNA (Pharmingen), and the transfer vectors were cotransfected by the Lipofectin-mediated method as specified by the manufacturer (Gibco BRL, Gaithersburg, MD). The cells were incubated at 26.5°C in TC-100 medium (Gibco BRL) supplemented with 8% fetal bovine serum and 0.26% Bacto tryptose phosphate broth (Difco Laboratories, Detroit, MI). The proteins in the culture medium and cell lysate were separated by sodium dodecyl sulfate-polyacrylamide gel electrophoresis (SDS-PAGE) and analyzed by Western blot assay using serum from a patient with acute hepatitis E (11). Each recombinant virus was plaque purified three times. The baculovirus recombinants thus obtained were designated as Ac[n111], Ac[n111c52], Ac[n111c58], Ac[n111c59], Ac[n111c60], Ac[n111c64], Ac[n111c72], Ac[c52], Ac[n123], Ac[n124], Ac[n125], Ac[n126], Ac[n130], and Ac[n125c59]; a schematic diagram is shown in Fig. 1. Both insect Sf9 and Tn5 cells, the latter from a *Trichoplusia ni* insect cell line, BTI-Tn-5B1-4 (Invitrogen, San Diego, CA), were infected with recombinant baculoviruses at a multiplicity of infection of 10 and incubated for 5 days at 26.5°C as previously described (11, 23).

Purification of VLPs. The culture medium was harvested on day 5 after infection. The intact cells, cell debris, and progeny baculoviruses were removed by centrifugation at 10,000 × g for 90 min. The supernatant was then spun at 25,000 rpm for 2 h in a Beckman SW28 rotor. The resulting pellet was resuspended in 4.5 ml EX-CELL 405 at 4°C overnight. After mixing with 1.96 g of CsCl, the sample was centrifuged at 35,000 rpm for 24 h at 4°C in a Beckman SW50.1 rotor. The visible white band (at a density of 1.285 g/ml) was harvested by puncturing the tubes with a 21-gauge needle, diluted with EX-CELL 405 medium, and then centrifuged again in a Beckman TLA45 rotor at 45,000 rpm (125,000 × g) for 2 h to remove CsCl. The VLPs were placed on a carbon-coated grid, and the proteins were allowed to be absorbed into the grid for 5 min. After being rinsed with distilled water, the sample was stained with a 1% aqueous uranyl acetate solution and examined with a Hitachi H-7000 electron microscope operating at 75 kV.

Terminal amino acid sequence analysis. The VLPs were further purified by 5 to ~30% sucrose gradient centrifugation at 35,000 rpm for 2 h in a Beckman SW50.1 rotor. The visible white band was harvested as described above, diluted with EX-CELL 405, and again centrifuged at 45,000 rpm for 2 h in a Beckman TLA55 rotor to precipitate the VLPs. N-terminal aa microsequencing was carried out using 100 pmol of the protein by Edman automated degradation on an Applied Biosystems model 477 protein sequencer, and C-terminal aa sequencing was performed by Applied Biosystems.

SDS-PAGE and Western blot analysis. Dispersed insect cells were incubated for 20 min at room temperature to allow the cells to attach to culture flasks in TC-100 (Sf9 cells) or EX-CELL 405 (Tn5 cells) medium. The culture medium was removed, and the cells were infected with the recombinant baculoviruses at
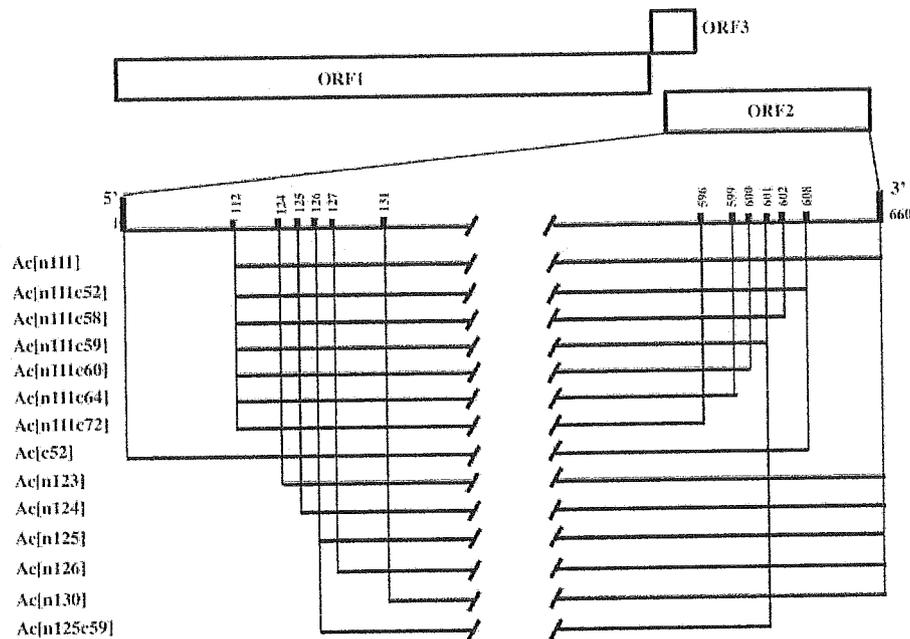
FIG. 1. Genome organization of HEV and schematic diagram of recombinant baculovirus vectors. DNA fragments encoding N- and C-terminal aa-truncated ORF2 were prepared by PCR with the primers listed in Table 1 and were used to construct 14 recombinant baculoviruses. Full-length pORF2 consisted of 660 aa. The N- and C-terminal aa numbers of the truncated protein are indicated.

a multiplicity of infection of 10. Virus adsorption was carried out for 1 h at room temperature, and then the cells were incubated at 26.5°C. The proteins in the cell lysate and in the culture medium were separated by 10% SDS-PAGE and stained with Coomassie blue. For Western blotting, the proteins in the SDS-PAGE gel were electrophoretically transferred onto a nitrocellulose membrane. The membrane was then blocked with 5% skim milk in 50 mM Tris-HCl (pH 7.4)–150 mM NaCl and reacted with a patient's serum from an acute phase. Human IgG antibody was detected by using alkaline phosphatase-conjugated goat anti-human immunoglobulin (1:1,000 dilution) (DAKO A/S, Copenhagen, Denmark). Nitroblue tetrazolium chloride and 5-bromo-4-chloro-3-indolyl phosphate P-toluidine were used as coloring agents (Bio-Rad Laboratories).

Cryo-electron microscopy (cryo-EM) and image reconstruction. A 3-μl drop of purified HEV VLP (~1 mg/ml) was applied onto holey carbon film. After extra solution was wiped away with filter paper, the grid was rapidly plunged into liquid ethane surrounded by liquid nitrogen. Thus embedded in a thin layer of vitrified ice, the specimen was then transferred via a Gatan 626 cryo-transfer system to a Philips CM120 microscope. The specimen was observed at liquid nitrogen temperature and photographed at a magnification of 45,000. Each area was photographed twice, with defocus levels of 1 μm and 3 μm, respectively. The electron dose of each exposure was less than 10 electrons/$Å^2$. The selected electron micrographs were digitized with a Zeiss scanner at a step size of 14 μm, corresponding to 3.1 Å at the specimen. The images were reconstructed according to icosahedral symmetry with Fourier-Basel procedures (4, 28). Briefly, the particle orientation and center of each image were estimated with the EMPFT program, where the structure of Tn5-produced HEV VLP was used as the initial model (1). The first reconstruction was generated from selected images and used as a model to refine the orientation and center parameters. After itinerant runs of EMPFT, the parameters were stable and appeared unchanged from one EMPFT run to another. The final reconstruction was computed by combining 353 images at a resolution of 23 Å. The surface-rendering map was generated with the NAG Explorer program combined with custom-created modules.

Mass spectrometry. The mass spectrometry experiment was done with a Reflex III mass spectrometer from Bruker, equipped with gridless delayed extraction. The samples were mixed with an equal volume of a saturated solution of sinapinic acid (Sigma Chemical Co., St. Louis, MO) in 33% (vol/vol) acetonitrile and 0.1% (vol/vol) trifluoroacetic acid. On the target plate, a thin layer was prepared with a saturated solution of sinapinic acid in ethanol. A sample volume of 0.5 μl was applied to a thin layer of sinapinic acid and allowed to crystallize. Data were acquired in the linear instrument mode. Data were processed and evaluated by XMASS software from Bruker.

RESULTS

C-terminal 52-amino-acid deletion is necessary for formation of VLPs in Sf9 cells. To understand the mechanism underlying VLP formation in Sf9 and Tn5 cells, we prepared a series of baculovirus recombinants expressing pORF2 with different deletions at the N- and/or C-terminal region (Table 1 and Fig. 1). The cell lysate and culture medium of infected insect cells were analyzed by Western blotting. In a previous study, the N-terminal 111 aa-truncated HEV pORF2 was expressed by a recombinant baculovirus, Ac[n111], in both insect cells (11). Two major proteins, ~58K and ~53K, were detected in both cell lysates. The 53K protein was released into cell culture medium and assembled into VLPs in Tn5 cells but not in Sf9 cells (11).

Analysis of the N- and C-terminal aa sequences of the VLPs revealed that the N terminus was at aa residue 112 and the C terminus ended at aa residue 608, indicating that the C-terminal 52 aa of ORF2 were deleted. The protein that forms VLPs contains 497 amino acids (112 to ~608), and its molecular mass was about 53K. An N-terminal 111 aa- and C-terminal 52 aa-truncated construct, Ac[n111c52], was generated, and the protein was expressed in both Sf9 and Tn5 cells. As expected, a single 53K protein was found in both Sf9 and Tn5 cell lysates (Fig. 2, Ac[n111c52] lanes in Sf9 and Tn5). Interestingly, these 53K proteins were released into both culture media as VLPs, as observed by electron microscopy (Fig. 3). The particle appeared empty and homogenous in size. Therefore, C-terminal truncation to aa residue 608 is crucial for particle formation and release into Sf9 cells.

Ac[n111c58] and Ac[n111c59] encode truncated pORF2s with an N-terminal 111-aa deletion and respective C-terminal deletions of 58 and 59 aa. The expressed proteins migrated to

FIG. 2. Western blot assay of truncated pORF2 expressed in Sf9 and Tn5 cells. Eight recombinant baculoviruses, Ac[n111], Ac[n111c52], Ac[n111c58], Ac[n111c59], Ac[n111c60], Ac[n111c64], Ac[n111c72], and Ac[c52], were used to infect the insect cells. Ten microliters of the culture medium (right column) and 5 μl of the cell lysate (left column) were separated by 10% SDS-PAGE, and HEV-specific proteins were detected by Western blot analysis using the serum of a patient with acute hepatitis E. M, molecular weight markers; W, wild-type baculovirus-infected cells.

a position similar to that of 53K and appeared in both cell lysates as well as in the culture medium (Fig. 2); both were also assembled into VLPs (data not shown). In contrast, truncated pORF2 from Ac[n111c60], Ac[n111c64], and Ac[n111c72] was not released into the culture medium to detectable levels, and VLP was not formed even though protein expression remained similar to those of the other constructs (Fig. 2). Instead, a

FIG. 3. EM of the HEV VLPs generated in Tn5 (A) and Sf9 (B) cells with recombinant baculovirus Ac[n111c52]. The VLPs were stained with 2% uranyl acetate. Bar, 100 nm.

protein with a molecular mass of 42 kDa was detected in both of the cell lysates as well as in the culture medium by Western blot analysis. When pORF2 with a C-terminal 52-aa deletion was expressed with a recombinant baculovirus, Ac[c52], two major proteins, 65K and ~53K, were observed in infected Tn5 and Sf9 cell lysates 5 days postinfection (p.i.). However, these two proteins were not detected in their culture media (Fig. 2, Ac[c52] lanes in Sf9 and Tn5). These results indicated that aa residues before 601 were essential to the formation of VLPs.

VLPs produced in Sf9 and Tn5 cells possess the same configurations and structures. The morphology of the VLPs generated in Sf9 cells appeared to be similar to that generated in Tn5 cells, as observed in the negatively stained particles (Fig. 3). To investigate the structural properties of these two released VLPs, we performed cryo-electron microscopy and image processing using VLPs produced in Tn5 cells. The electron cryomicrographs showed that the particle projected as a spiky hollow sphere, indicating that no RNA-like density was packed inside the capsid (Fig. 4A). The image processing was done according to the icosahedral procedure. The rotational symmetry of 522 was applied to reconstruct the final three-dimensional structure. The reconstructed VLP displayed a T=1 surface lattice with protruding density located at each of 30 twofold axes (Fig. 4B). The VLP was composed of 60 copies of pORF2, and the protruding density consisted of dimeric, projecting domains from twofold-related peptides. The particle diameter was 270 Å, measured from the three-dimensional reconstruction. The protein shell was 85 Å thick at the twofold axes. A channel can be observed under each protruding density. The protruding density was about 43 Å high, and the twofold platform was 56 Å in the long axes (data not shown). The threefold-related dimers formed a regular triangle, and the dimer-dimer distance was 76 Å measured from center to center (Fig. 4B). Molecular interactions at the icosahedral threefold region appeared much stronger than those at the fivefold region. There was no significant difference in radial density distribution between Tn5- and Sf9-produced VLPs (Fig. 4C).

We further determined the composition of the particles obtained from Sf9 and Tn5 cells using mass spectrometry (Fig. 5). HEV VLPs produced from Tn5 and Sf9 cells with recombinant baculovirus Ac[n111c52] were analyzed. In both cases, the major density peak was monitored at the position corresponding to a mass of 53 kDa. The peak was symmetrically distributed, and a shoulder tip can be found in both cases. The shoulder tip was about 1 kDa larger than the main density peak. The signals further confirmed that the molecular mass of truncated pORF2 was 53 kDa, disregarding the production cell lines.

Essential N-terminal amino acids for VLP formation. Deletion of the N-terminal 111 residues is necessary for particle formation, which is consistent with our previous observation (11). The subsequent question is how many amino acids can be removed from pORF2 N termini without changing its capability to form VLPs. We made five constructs to express proteins with 123-, 124-, 125-, 126-, and 130-aa deletions at the N terminus by using five recombinant baculoviruses: Ac[n123], Ac[n124], Ac[n125], Ac[n126], and Ac[n130], respectively. As shown in Fig. 6, three proteins, having molecular masses of 58 to 51 kDa, were detected by Western blotting in both cell lysates at 5 days p.i., and the largest bands (58 to ~57K) were
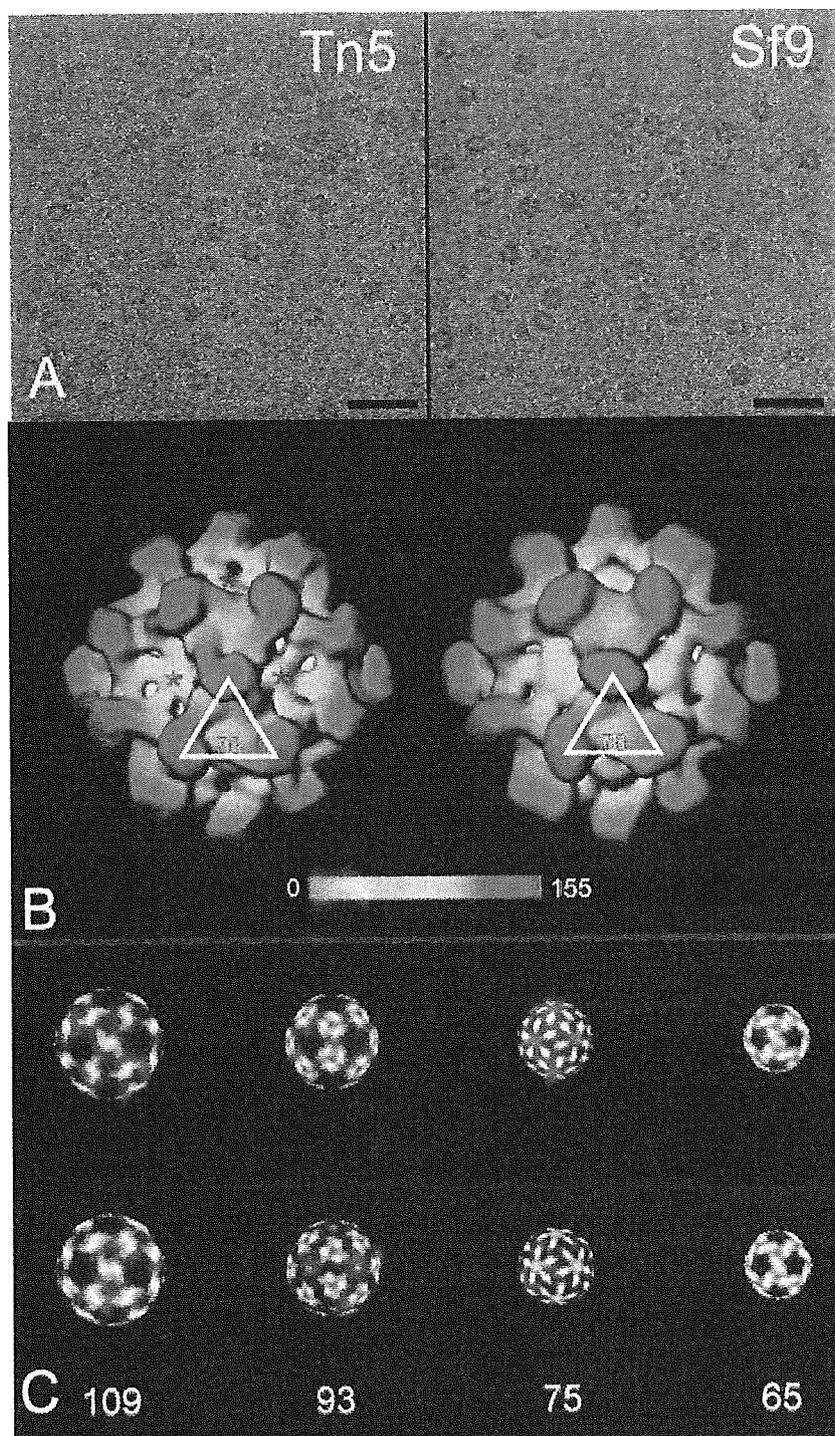
FIG. 4. HEV VLP structures determined by cryo-electron microscopy and image reconstruction. (A) Cryo-electron micrograph of ice-embedded HEV VLPs produced from Tn5 and Sf9 cells. The bar corresponds to 100 nm. (B) Surface-shaded representation of HEV VLP structures viewed along icosahedral twofold axes. VLPs from both Tn5 (left panel) and Sf9 (right panel) cells were color coded according to the radius, as indicated in the scale bar. The adjacent protruding spikes remain at equal distances of 76Å (white lines). The asterisks mark the positions of three adjacent icosahedral fivefold axes. (C) Sequential radial density projections generated from the twofold-oriented density map at corresponding radii. The protein density appears as the light color, while the background density is black.

thought to be the primary translation products encoded by N-terminal 123, 124, 125, 126, and 130 aa-truncated ORF2. In Tn5 cells, a C-terminal 52-aa-deleted product, about 51K protein, was the major protein to be efficiently released into the culture medium, where VLP formation occurred in Ac[n123]-, Ac[n124]-, and Ac[n125]-infected Tn5 cells (data not shown). Although the 51K protein was released into the culture medium, no VLP formation occurred in Ac[n126]- or Ac[n130]-
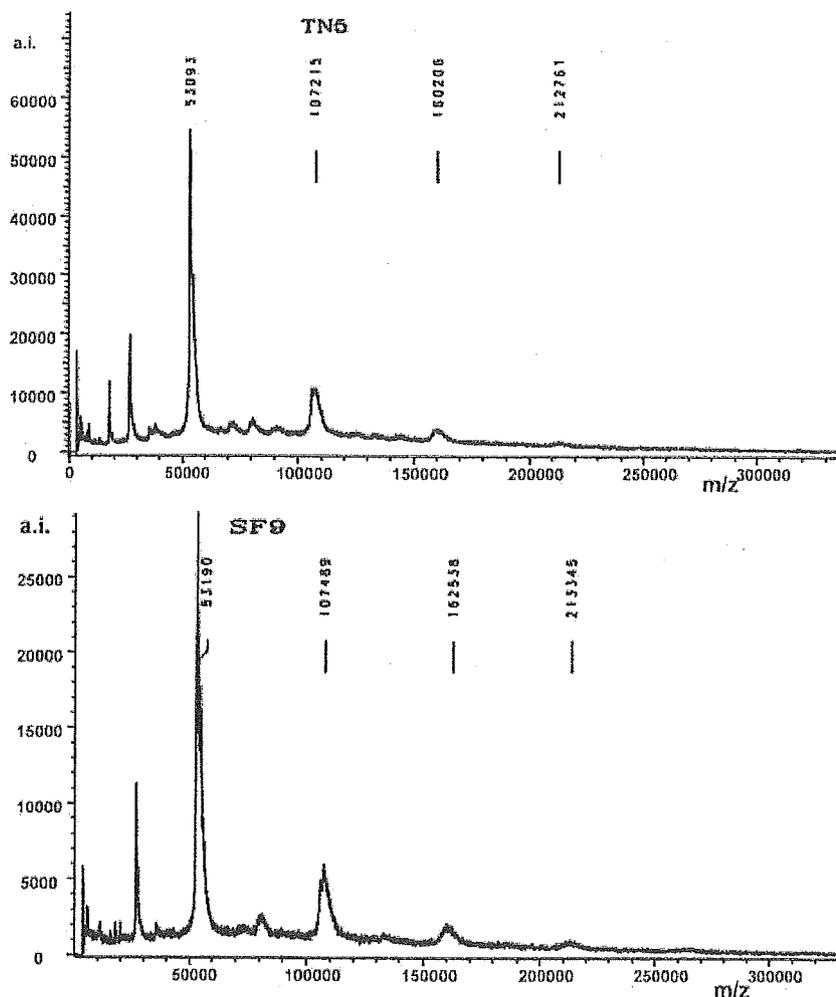
FIG. 5. Mass spectra from purified HEV VLPs displayed as the counts of isotope abundance (a.i.) versus mass/charge values (*m/z*). HEV VLPs produced from Tn5 (top panel) and Sf9 (bottom panel) cells with recombinant baculovirus Ac[n111c52] gave consistent mass spectra in which the abundant elements show similar *m/z* values at 53,000, 107,000, and 160,000.

infected Tn5 cells. In contrast, the 51K protein was not re-leased into the culture medium in infected Sf9 cells (Fig. 6). These results demonstrated that aa residues after 125 were essential to the formation of VLPs.

When Ac[n125c59], an N-terminal 125 aa- and C-terminal 59 aa-truncated recombinant baculovirus, was expressed in Sf9 and Tn5 cells, the 51K protein was detected in both cell lysates and the culture media, where VLP formation occurred in both insect cell types (Fig. 6). This confirmed our observation that a C-terminal deletion of 52 to 59 amino acids was required for particle formation when Sf9 cells were used.

DISCUSSION

HEV is enigmatic due to the virus's inability to grow in conventional cell culture. Large quantities of the HEV capsid protein carrying antigenicity and immunogenicity comparable to those of the native virion have been generated for a long time, because the capsid protein is a key molecule for the diagnosis of hepatitis E as well as for vaccine development.

We previously found that when an N-terminal 111 aa-trun-

cated ORF2 protein was expressed in Tn5 and Sf9 cells, two major peptides, having molecular masses of 58 and 53 kDa, were generated in both cells, and only the 53-kDa protein generated in Tn5 cells was released into culture medium and self-assembled into VLPs (11). The 58K protein presented the primary translation product, and the 53K protein is a process-ing product from the 58K protein. In this study, we examined the difference between Tn5 and Sf9 cells in HEV ORF2 gene expression and found that when a recombinant baculovirus (Ac[n111c52]) harboring a construct of the C-terminal 52-aa deletion was used, no difference between Sf9 and Tn5 cells in protein translation and particle formation was found. The ob-servation that Ac[n111] failed to produce VLPs in Sf9 cells raised a question about the posttranslation modification in insect cells. In Tn5 cells, the levels of protein expression by Ac[n111] and Ac[n111c52] appeared to be similar. Therefore, it is likely that the 58K protein was incorrectly processed in Sf9 cells, thus affecting VLP assembly.

In addition, when Sf9 insect cells were infected with Ac[n111], the expressed proteins were localized in the cyto-
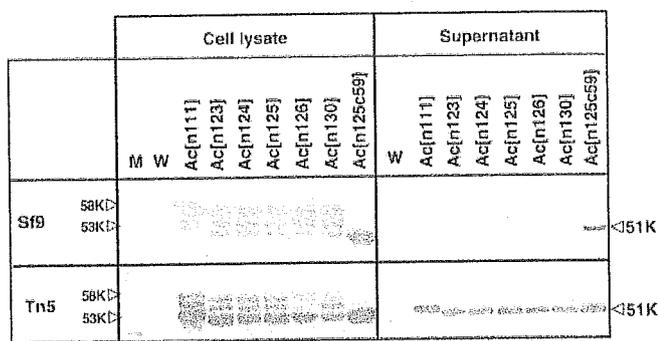
FIG. 6. Expression of N-terminally truncated pORF2 in Sf9 and Tn5 cells infected with Ac[n123], Ac[n124], Ac[n125], Ac[n126], Ac[n130], and Ac[n125c59]. A Western blot assay was carried out as described in the legend to Fig. 2. Ac[n111] was included for the expression of the 58K and 53K proteins. M, molecular weight markers; W, wild-type baculovirus-infected cells.

plasm and observed as inclusion-like bodies (one to four structures per cell) by EM (25). In contrast, when Sf9 cells were infected with Ac[n111c52], there were no inclusion-like bodies (data not shown), and the expressed proteins were localized evenly in the cytoplasm. Concomitantly, expressed protein was poorly detected in the culture medium from Ac[n111]-infected Sf9 cells at 3 days p.i., whereas a large amount of the 53K protein was detected in the culture medium from Ac[n111c52]-infected Sf9 cells. These findings suggest that the C-terminal aa of ORF2 might affect the localization, and subsequently the release, of the capsid protein from the insect cells. However, we do not yet know whether the VLPs form before release in infected cells or after release in culture medium.

The presence of Leu601 in pORF2 is important for the formation of HEV VLPs. A protein with a longer (580 to 610) deletion of aa residues was aberrant in protein folding; this may reduce the ORF2 homo-oligomerization (24). The prediction of the secondary structure based on protein sequence suggests two β-strand motifs in the region between aa 580 and 601 (580 to ~589 and 593 to ~601). The failure in the particle assembly with Ac[n111c60] is due to incomplete formation of this β-strand motif. Although aa 111 to 601 and aa 111 to 602 formed VLPs, the yield of each of these was about 10 to 20% of the yields of aa 111 to 660 (data not shown). This is in contrast to the fact that the levels of protein expression inside the cells were similar in these constructs. This observation further confirmed that stability of the C-terminal β-strand motif is essential for VLP assembly.

The N-terminal 111-aa-deletion was found to be essential for cellular membrane dissociation of pORF2 expressed in insect cells (17, 24). We extended the N-terminal deletion up to Val125 without altering the ability to form HEV VLPs (Fig. 6). The ORF2 protein exhibits two-domain folding (25), with a domain organization similar to those of the norovirus (NV) capsid protein (15) and the tomato bushy stunt virus capsid protein (14). The N-terminal aa residues 112 to 125 may be the arm region extending from the S domain into the particle interior. In NV, the N-terminal region appeared to serve as a switch controlling the S domain configuration in the assembly process (3). Removal of the first 20 amino acids did not affect NV-like particle self-assembly, but a longer deletion at the

N-terminal region did (3). Thus, residues 112 to 125 are putatively located in the HEV virion interior and may regulate VLP assembly.

Tn5 and Sf9 are insect cell lines that are commonly used in recombinant protein expression. The Tn5 cell is becoming more and more popular because it yields higher quantities of tissue factor than Sf9. Under optimum conditions, Tn5 cells produce 28-fold more secreted soluble tissue factor than Sf9 cells on a per-cell basis (23). In this paper, we report the difference between Tn5 and Sf9 cells in a protein synthesis system. The ORF2 protein underwent posttranslation cleavage, which is crucial for HEV VLP assembly. Although the HEV virion assembly mechanism remains unclear, our data indicate that the region consisting of ORF2 residues 126 to 601 is the kernel element for the monomer-monomer interaction and thus initiates VLP assembly.

Recombinant HEV VLPs themselves can be candidates for parenteral as well as oral hepatitis E vaccines (9, 10), and these VLPs have potential as mucosal vaccine carrier vehicles for the presentation of foreign antigenic epitopes through oral administration (13). Furthermore, HEV VLPs can be a vector for gene delivery to mucosal tissue for the purposes of DNA vaccination and gene therapy (20). The results of the present study provide the basic tool to construct VLPs having novel functions.

REFERENCES

1. **Baker, T. S., and R. H. Cheng.** 1996. A model-based approach for determining orientations of biological macromolecules imaged by cryoelectron microscopy. J. Struct. Biol. **116:**120–130.
2. **Balayan, M. S., A. G. Andjaparidze, S. S. Savinskaya, E. S. Ketiladze, D. M. Braginsky, A. P. Savinov, and V. F. Poleschuk.** 1983. Evidence for a virus in non-A, non-B hepatitis transmitted via the fecal-oral route. Intervirology **20:**23–31.
3. **Bertolotti-Ciarlet, A., L. J. White, R. Chen, B. V. Prasad, and M. K. Estes.** 2002. Structural requirements for the assembly of Norwalk virus-like particles. J. Virol. **76:**4044–4055.
4. **Cheng, R. H.** 2000. Visualization on the grid of virus-host interactions, p. 141–153. *In* L. Johnsson (ed.), Simulation and visualization on the grid. Springer-Verlag, New York, N.Y.
5. **He, J., A. W. Tam, P. O. Yarbough, G. R. Reyes, M. Carl, P. O. Yarbough, A. W. Tam, K. E. Fry, K. Krawczynski, K. A. McCaustland, D. W. Bradley, and G. R. Reyes.** 1993. Expression and diagnostic utility of hepatitis E virus putative structural proteins expressed in insect cells. J. Clin. Microbiol. **31:**2167–2173.
6. **Kar-Roy, A., H. Korkaya, R. Oberoi, S. K. Lal, and S. Jameel.** 2004. The hepatitis E virus open reading frame 3 protein activates ERK through binding and inhibition of the MAPK phosphatase. J. Biol. Chem. **279:**28345–28357.
7. **Koonin, E. V., A. E. Gorbalenya, M. A. Purdy, M. N. Rozanov, G. R. Reyes, and D. W. Bradley.** 1992. Computer-assisted assignment of functional domains in the nonstructural polyprotein of hepatitis E virus: delineation of an additional group of positive-strand RNA plant and animal viruses. Proc. Natl. Acad. Sci. USA **89:**8259–8263.
8. **Korkaya, H., S. Jameel, D. Gupta, S. Tyagi, R. Kumar, M. Zafrullah, M. Mazumdar, S. K. Lal, L. Xiaofang, D. Sehgal, S. R. Das, and D. Sahal.** 2001.

The ORF3 protein of hepatitis E virus binds to Src homology 3 domains and activates MAPK. J. Biol. Chem. **276:**42389–42400.

9. Li, T. C., N. Takeda, and T. Miyamura. 2001. Oral administration of hepatitis E virus-like particles induces a systemic and mucosal immune response in mice. Vaccine **19:**3476–3484.

10. Li, T. C., Y. Suzaki, Y. Ami, T. N. Dhole, T. Miyamura, and N. Takeda. 2004. Protection of cynomolgus monkeys against HEV infection by oral administration of recombinant hepatitis E virus-like particles. Vaccine **22:**370–377.

11. Li, T. C., Y. Yamakawa, K. Suzuki, M. Tatsumi, M. A. Razak, T. Uchida, N. Takeda, and T. Miyamura. 1997. Expression and self-assembly of empty virus-like particles of hepatitis E virus. J. Virol. **71:**7207–7213.

12. Magden, J., N. Takeda, T. C. Li, P. Auvinen, T. Ahola, T. Miyamura, A. Merits, and L. Kaariainen. 2001. Virus-specific mRNA capping enzyme encoded by hepatitis E virus. J. Virol. **75:**6249–6255.

13. Niikura, M., S. Takamura, G. Kim, S. Kawai, M. Saijo, S. Morikawa, I. Kurane, T. C. Li, N. Takeda, and Y. Yasutomi. 2002. Chimeric recombinant hepatitis E virus-like particles as an oral vaccine vehicle presenting foreign epitopes. Virology **293:**273–280.

14. Olson, A. J., G. Bricogne, and S. C. Harrison. 1983. Structure of tomato busy stunt virus. IV. The virus particle at 2.9 A resolution. J. Mol. Biol. **171:**61–93.

15. Prasad, B. V., M. E. Hardy, T. Dokland, J. Bella, M. G. Rossmann, and M. K. Estes. 1999. X-ray crystallographic structure of the Norwalk virus capsid. Science **286:**287–290.

16. Purcell, R. H., and S. U. Emerson. 2001. Hepatitis E virus, p. 3051–3061. *In* D. M. Knipe and P. M. Howley (ed.), Fields virology, 4th ed., vol. 1. Lippincott Williams & Wilkins, Philadelphia, Pa.

17. Robinson, R. A., W. H. Burgess, S. U. Emerson, R. S. Leibowitz, S. A. Sosnovtseva, S. Tsarev, and R. H. Purcell. 1998. Structural characterization of recombinant hepatitis E virus ORF2 proteins in baculovirus-infected insect cells. Protein Expr. Purif. **12:**75–84.

18. Schofield, D. J., J. Glamann, S. U. Emerson, and R. H. Purcell. 2000. Identification by phage display and characterization of two neutralizing chimpanzee monoclonal antibodies to the hepatitis E virus capsid protein. J. Virol. **74:**5548–5555.

19. Stewart, L. M. D., and R. D. Possee. 1993. Baculovirus expression vectors, p. 227–256. *In* A. J. Davidson and R. M. Elliotts (ed.), Molecular virology: a practical approach. IRL Press, Oxford, United Kingdom.

20. Takamura, S., M. Niikura, T. C. Li, N. Takeda, S. Kusagawa, Y. Takebe, T. Miyamura, and Y. Yasutomi. 2004. DNA vaccine-encapsulated virus-like particles derived from an orally transmissible virus stimulate mucosal and systemic immune responses by oral administration. Gene Ther. **11:**628–635.

21. Tam, A. W., M. M. Smith, M. E. Guerra, C. C. Huang, D. W. Bradley, K. E. Fry, and G. R. Reyes. 1991. Hepatitis E virus (HEV): molecular cloning and sequencing of the full-length viral genome. Virology **185:**120–131.

22. Virus Taxonomy. 2002. http://www.ictvdb.iacr.ac.uk/Ictv/fr-fst-g.htm.

23. Wickham, T. J., and G. R. Nemerow. 1993. Optimization of growth methods and recombinant protein production in BTI-Tn-5B1-4 insect cells using the baculovirus expression system. Biotechnol. Prog. **9:**25–30.

24. Xiaofang, L., M. Zafrullah, F. Ahmad, and S. Jameel. 2001. A C-terminal hydrophobic region is required for homo-oligomerization of the hepatitis E virus capsid (ORF2) protein. J. Biomed. Biotechnol. **1:**122–128.

25. Xing, L., K. Kato, T. Li, N. Takeda, T. Miyamura, L. Hammar, and R. H. Cheng. 1999. Recombinant hepatitis E capsid protein self-assembles into a dual-domain T = 1 particle presenting native virus epitopes. Virology **265:** 35–45.

26. Yarbough, P. O., A. W. Tam, K. E. Fry, K. Krawczynski, K. A. McCaustland, D. W. Bradley, and G. R. Reyes. 1991. Hepatitis E virus: identification of type-common epitopes. J. Virol. **65:**5790–5797.

27. Zafrullah, M., M. H. Ozdener, S. K. Panda, and S. Jameel. 1997. The ORF3 protein of hepatitis E virus is a phosphoprotein that associates with the cytoskeleton. J. Virol. **71:**9045–9053.

28. Zhong, Y., J. Cheng, Y. Liu, J. Dong, J. Yang, and L. Zhang. 2000. Expression of human single-chain variable fragment antibody against non-structural protein 3 of hepatitis C virus antigen in e. coli. Zhonghua Gan Zang Bing Za Zhi **8:**171–173. (In Chinese.)

Involvement of the Toll-Like Receptor 9 Signaling Pathway in the Induction of Innate Immunity by Baculovirus†

Takayuki Abe,[1] Hiroaki Hemmi,[2] Hironobu Miyamoto,[1] Kohji Moriishi,[1] Shinichi Tamura,[3] Hiroshi Takaku,[4] Shizuo Akira,[2] and Yoshiharu Matsuura[1]*

Research Center for Emerging Infectious Diseases,[1] Department of Host Defense,[2] and Laboratory of
Prevention of Viral Diseases,[3] Research Institute for Microbial Diseases, Osaka University,
Osaka, and Department of Industrial Chemistry and High Technology
Research Center, Chiba Institute of Technology, Chiba,[4] Japan

We have previously shown that mice inoculated intranasally with a wild-type baculovirus (*Autographa californica* nuclear polyhedrosis virus [AcNPV]) are protected from a lethal challenge by influenza virus. However, the precise mechanism of induction of this protective immune response by the AcNPV treatment remained unclear. Here we show that AcNPV activates immune cells via the Toll-like receptor 9 (TLR9)/ MyD88-dependent signaling pathway. The production of inflammatory cytokines was severely reduced in peritoneal macrophages (PECs) and splenic CD11c$^+$ dendritic cells (DCs) derived from mice deficient in MyD88 or TLR9 after cultivation with AcNPV. In contrast, a significant amount of alpha interferon (IFN-α) was still detectable in the PECs and DCs of these mice after stimulation with AcNPV, suggesting that a TLR9/MyD88-independent signaling pathway might also participate in the production of IFN-α by AcNPV. Since previous work showed that TLR9 ligands include bacterial DNA and certain oligonucleotides containing unmethylated CpG dinucleotides, we also examined the effect of baculoviral DNA on the induction of innate immunity. Transfection of the murine macrophage cell line RAW264.7 with baculoviral DNA resulted in the production of the inflammatory cytokine, while the removal of envelope glycoproteins from viral particles, UV irradiation of the virus, and pretreatment with purified baculovirus envelope proteins or endosomal maturation inhibitors diminished the induction of the immune response by AcNPV. Together, these results indicate that the internalization of viral DNA via membrane fusion mediated by the viral envelope glycoprotein, as well as endosomal maturation, which releases the viral genome into TLR9-expressing cellular compartments, is necessary for the induction of the innate immune response by AcNPV.

The baculovirus *Autographa californica* nuclear polyhedrosis virus (AcNPV) has long been used as a biopesticide and as an efficient tool for recombinant protein production in insect cells (39, 42). Subsequently, its efficacy for the delivery of high-level expression of foreign genes under the control of mammalian promoters in infected mammalian cells was also demonstrated (12, 26, 48). Since it causes no visible cytopathic effects, even at high titers, and does not replicate in mammalian cells (49), this baculovirus is now recognized as a useful viral vector, not only for the expression of foreign proteins in insect cells, but also for gene delivery to mammalian cells (4, 9, 12, 16, 26, 28, 37, 45, 48, 49, 53, 54).

AcNPV was also shown to be capable of stimulating interferon (IFN) production in mammalian cell lines and can confer protection from lethal encephalomyocarditis virus infections in mice (18). We demonstrated that intranasal inoculation with AcNPV induces a strong innate immune response and protects mice from a lethal challenge of influenza A and B viruses (1). Furthermore, inoculation with baculovirus induces the secretion of inflammatory cytokines, such as tumor necrosis factor

alpha (TNF-α), interleukin-6 (IL-6), and IL-12, in RAW264.7, a murine macrophage cell line. However, the precise mechanism of induction of the protective immune response by a pretreatment with AcNPV remained unclear.

Members of the IL-1 receptor/Toll-like receptor (TLR) superfamily are key mediators of innate and adaptive immunity (5). Toll, the first member of this superfamily to be identified, was initially discovered as a factor involved in dorsoventral axis formation in fly embryos and was later shown to participate in host defense mechanisms (38). A family of TLRs exists in mammals and has been shown to play an important role not only in the recognition of a wide variety of infectious pathogens and their products, but also in protection of the host from infections with pathogens. So far, 11 TLR family members and their corresponding ligands have been identified, with TLR1 being the only orphan receptor among them. Different TLRs have been shown to mediate immune responses to a variety of different pathogen-derived elements. For example, TLR4, TLR5, and TLR9 are essential for the recognition of lipopolysaccharides (LPS), bacterial flagellin, and bacterial DNA containing unmethylated CpG motifs, respectively (21, 24, 27, 46). TLR2 is implicated in the recognition of peptidoglycan (PGN) and lipopeptides (7, 13, 50, 57), while TLR6 can associate with TLR2 and recognize PGN and lipopeptides derived from mycoplasma (44). On the other hand, TLR3 has been shown to activate immune cells in response to virus-derived double-stranded RNA (6). Although synthetic imidazoquinoline com-

* Corresponding author. Mailing address: Research Center for Emerging Infectious Diseases, Research Institute for Microbial Diseases, Osaka University, 3-1 Yamada-oka, Suita, Osaka 565-0871, Japan. Phone: 81-6-6879-8340. Fax: 81-6-6879-8269. E-mail: matsuura @biken.osaka-u.ac.jp.

pounds and guanosine analogs with antiviral activities have been shown to activate TLR7 and TLR8 (25, 36), it was recently demonstrated that single-stranded RNAs from RNA viruses are the natural ligands of these receptors (17, 23). The most recently identified TLR, termed TLR11, senses bacteria that cause infections of the bladder and kidney (60). In summary, TLRs recognize specific components derived from pathogens and activate a signaling cascade that causes proinflammatory cytokine production and subsequent immune responses.

TLRs share a common cytoplasmic Toll–IL-1 receptor (TIR) domain. MyD88, also a TIR domain-containing protein, associates with TLRs and acts as an adapter that recruits IL-1 receptor-associated kinase and TNF receptor-associated factor 6 (TRAF6) to TLRs. Macrophages isolated from MyD88-deficient mice fail to activate NF-κB and Jun N-terminal protein kinase or to produce inflammatory cytokines in response to microbial components such as lipopeptides, LPS, and CpG-rich bacterial DNA (20, 52), indicating that MyD88 is a critical component in the signaling pathway that leads to the production of inflammatory cytokines.

Viruses are obligate intracellular parasites; accordingly, viral proteins synthesized in host cells bear modifications that reflect the identity and characteristics of the host. Therefore, viral particles do not display exclusively pathogen-associated molecular patterns. Although the mechanisms by which the innate immune response is induced by viral infection are poorly understood, there is increasing evidence suggesting that TLRs function to detect viruses and trigger inflammatory responses. For instance, respiratory syncytial virus and mouse mammary tumor virus activate innate immunity through TLR4 (22, 34, 47), which is a signaling receptor for LPS. Similarly, hemagglutinin from wild-type measles virus was reported to activate TLR2 (10), which also recognizes certain elements of gram-positive bacteria and fungi. Herpes simplex virus type 1 (HSV-1) and human cytomegalovirus have also been shown to recognize TLR2 (15, 35), while vaccinia virus encodes proteins containing amino acid sequences similar to the Toll/IL-1 receptor domain and inhibits IL-1-, IL-18-, and TLR4-mediated signal transduction (11).

It was recently shown that HSV-1 and -2, whose genomes contain abundant CpG motifs, can induce angiogenesis and a variety of diseases, including herpes stromal keratitis, that produce chronic inflammatory responses via a TLR9/MyD88-dependent signaling pathway (33, 40, 61). HSV-1 and -2 are also able to trigger alpha interferon (IFN-α) secretion from plasmacytoid dendritic cells through TLR9/MyD88-dependent signaling (33, 40). The TLR9-mediated recognition of HSV by immunocompetent cells suggests that this recognition pathway may be important for the recognition of other DNA viruses.

For this study, we characterized the innate immune response induced by AcNPV. Peritoneal macrophages and splenic CD11c$^+$ dendritic cells obtained from TLR9 or MyD88 knockout mice exhibited severe reductions in proinflammatory cytokine production following stimulation with AcNPV, whereas a significant amount of IFN-α was still detectable in these cells. In addition, the frequency of CpG motifs in the AcNPV genome was similar to that of bacterial DNA and significantly higher than that of mammalian DNA. Furthermore, stimulation by AcNPV was eliminated by a treatment with inhibitors

of endosomal acidification. These results indicate that the internalization of viral AcNPV DNA via membrane fusion by envelope glycoproteins found in the endosome is required for the induction of a TLR9/MyD88-dependent innate immune response.

MATERIALS AND METHODS

Mice and cell culture. C57BL/6 mice were purchased from Clea Japan, Inc., Tokyo, Japan. MyD88-deficient (MyD88$^{-/-}$) mice were established as previously described (2) and backcrossed more than eight times with C57BL/6 mice. TLR9$^{-/-}$ mice were generated as previously described (24). The mice were injected intraperitoneally with 2 ml of 4% thioglycolate (Sigma-Aldrich Co., St. Louis, Mo.), and cells were harvested 3 days later by peritoneal lavage. The mouse macrophage cell line RAW264.7 was purchased from Riken Cell Bank (Tsukuba, Japan) and maintained in Dulbecco's modified Eagle's medium (Sigma-Aldrich) supplemented with 10% (vol/vol) heat-inactivated fetal calf serum (FCS), 1.5 mM L-glutamine, 100 U of penicillin/ml, and 100 μg of streptomycin/ml at 37°C in a 5% CO_2 humidified incubator.

Viruses and reagents. AcNPV was propagated in *Spodoptera frugiperda* (Sf-9) cells in Sf-900II insect medium supplemented with 10% (vol/vol) heat-inactivated FCS. A mutant baculovirus, AcNPVΔ64, which lacks the gp64 envelope protein and possesses the green fluorescent protein gene under the control of the polyhedrin promoter in the gp64 gene locus, was generated (Y. Kitagawa et al., unpublished data). AcNPV and AcNPVΔ64 were purified as previously described (1). The inactivation of AcNPV was performed with a Stratalinker 2400 (Stratagene, La Jolla, Calif.) using short-wavelength UV radiation (UVC, 254 nm) at a distance of 5 cm for 30 min on ice (1.6 × 10^4 mJ/cm^2). The inactivation of infectivity was verified by a plaque assay with Sf-9 cells.

AcNPV DNA was isolated from the purified virions by a treatment with 10 mg of proteinase K (Sigma-Aldrich)/ml and 10% sodium dodecyl sulfate (SDS) in sterile phosphate-buffered saline (PBS) for 2 h at 55°C. The viral DNA was purified by phenol-chloroform-isoamyl alcohol extraction, precipitated at 12,000 × g, and resuspended in sterile endotoxin-free Tris-buffered saline. RNAs were removed by incubation with RNase A (10 mg/ml) (Wako Pure Chemical Industries, Osaka, Japan) for 1 h at 37°C, and the viral DNA was extracted as described above. The resultant DNA exhibited a single band by electrophoresis, and neither protein nor chromosomal DNA of insect cells was detected.

Phosphorothioate-stabilized mouse CpG (mCpG) oligodeoxynucleotides (ODN1668) (TCC-ATG-ACG-TTC-CTG-ATG-CT) and human CpG (hCpG) oligodeoxynucleotides (ODN2006) (TCG-TCG-TTT-TGT-CGT-TTT-GTC-GTT) were purchased from Invitrogen (Tokyo, Japan). Guanosine, 2'-deoxy-G, 8-bromo-G, 7-methyl-G, 7-allyl-8-oxo-G (loxoribine) was purchased from Invivogen (San Diego, Calif.). LPS derived from *Salmonella enterica* serovar Minnesota (Re-595), PGN derived from *Staphylococcus aureus*, monodansylcadaverine (MDC), and chloroquine were purchased from Sigma-Aldrich. Bafilomycin A1 and ammonium chloride were purchased from Wako Pure Chemical Industries. An anti-p39 mouse monoclonal antibody was kindly provided by G. F. Rohrmann. The virus stocks and the other TLR ligands were free of endotoxin (<0.01 endotoxin units/ml), as determined by use of a Pyrodick endotoxin measure kit (Seikagaku Co., Tokyo, Japan).

Production of authentic and truncated forms of gp64 proteins. cDNAs encoding a deletion mutant of gp64 lacking the transmembrane region (gp64ΔTM) as well as a wild-type version of gp64 were obtained by PCRs with AcNPV DNA as a template. The same 5' primer (5'-CATAAGCTTATGGTAAGCGCTATT GTTTTATAT-3') was used to amplify the gp64 and gp64ΔTM cDNAs, and the 3' primers were 5'-GATTCTAGAATATATTGTCTATTACGGTTTCT-3' and 5' GATTCTAGAATCGAAGTCAATTTAGCGGCCAA-3', respectively. cDNAs were subcloned into HindIII and XbaI sites in pIB/V5-His (Invitrogen). The sequences of the recombinant plasmids, pIBgp64/V5-His and pIBgp64ΔTM/V5-His, were confirmed by DNA sequencing. These plasmids were transfected into Sf-9 cells by the use of Unifector (B-Bridge International, Inc., San Jose, Calif.). After 3 days of incubation, the recombinant gp64 proteins were purified from cell lysates or supernatants by use of a column of nickel-nitrilotriacetic acid beads (QIAGEN, Valencia, Calif.). The protein concentrations were determined by use of a Micro BCA protein assay kit (Pierce, Rockford, Ill.). The recombinant proteins were analyzed by SDS–12.5% polyacrylamide gel electrophoresis (SDS–12.5% PAGE) under reducing conditions, stained with GelCord Blue staining reagent (Pierce), and detected by immunoblotting analysis with an antihexahistidine monoclonal antibody (Santa Cruz Biotechnology, Santa Cruz, Calif.).

Isolation of peritoneal cells and cytokine production. To evaluate cytokine production from macrophages in vitro, we seeded thioglycolate-elicited perito-

neal cells (PECs) into 96-well plates at a concentration of 2×10^5 cells/well and stimulated them with various doses of AcNPV and loxoribine. After 24 h of incubation, the culture supernatants were collected and analyzed for cytokine production. The concentrations of IL-12 p40 and IFN-α in culture supernatants were determined by enzyme-linked immunosorbent assays (ELISAs). ELISA kits for OptEIA mouse IL-12 p40 Set and mouse IFN-α were purchased from BD PharMingen (San Diego, Calif.) and PBL Biomedical Laboratories (New Brunswick, N.J.), respectively. Total RNAs were isolated by the use of Sepazol-RNA I (Nacalai Tesque, Kyoto, Japan), electrophoresed, and transferred to nylon membranes. Hybridization was performed with the indicated cDNA probes as previously described (2). cDNA probes specific for IL-12 p40 were established as previously described (31). To determine the effects of infection with AcNPV on cytokine production, we seeded the mouse macrophage cell line RAW264.7 into six-well plates at a concentration of 10^6 cells/well and stimulated them with various TLR ligands, with or without endosomal inhibitors such as chloroquine, bafilomycin A1, MDC, and ammonium chloride. For cell stimulation, AcNPV (5 μg/ml), LPS (10 ng/ml), PGN (2.5 μg/ml), and mCpG (200 ng/ml) were used.

Preparation of splenic dendritic cells and cytokine secretion. To prepare splenocytes containing dendritic cells (DCs), we cut spleen tissues into small fragments and incubated them with RPMI 1640 containing 400 U of collagenase (Wako)/ml and 15 μg of DNase (Sigma-Aldrich)/ml at 37°C for 20 min. For the last 5 min, 5 mM EDTA was added, and single-cell suspensions were prepared after red blood cell lysis. CD11c$^+$ cells were purified by magnetic cell sorting with anti-CD11c microbeads (Miltenyi Biotec GmbH, Bergisch Gladbach, Germany) according to the manufacturer's instructions and were used as splenic DCs. Enriched cells containing >90% CD11c$^+$ cells were seeded into 96-well plates at a concentration of 10^5 cells/well and stimulated with various doses of AcNPV or loxoribine. Culture supernatants were collected, and the production of IL-12 p40 and IFN-α was determined by ELISAs.

Indirect immunofluorescence assay and flow cytometric analysis. 293T cells transfected with a plasmid encoding human TLR9 were dislodged with PBS containing 5 mM EDTA 48 h after transfection. The cells were incubated with PBS containing 2% FCS and an anti-Flag (M2) monoclonal antibody (1:1,000) (Santa Cruz Biotechnology) for 1 h at 4°C, washed twice with PBS containing 2% FCS, and further incubated with fluorescein isothiocyanate-conjugated goat anti-mouse immunoglobulin G (IgG) (Sigma-Aldrich) in PBS containing 2% FCS for 1 h at 4°C. The cells were then fixed with 4% paraformaldehyde for 20 min, and the surface expression of human TLR9 was observed by fluorescence microscopy (UFX-II microscope; Nikon, Tokyo, Japan). Intracellular staining was examined after permeabilization with 0.5% Triton X-100. Stained cells were also analyzed by flow cytometry with a FACSCalibur instrument (Becton Dickinson, San Jose, Calif.), and the data were analyzed with CellQuest software (Becton Dickinson).

NF-κB–luciferase reporter gene assays with 293T cells. 293T cells were transfected with an NF-κB-dependent luciferase reporter plasmid (pELAM-Luc) together with human TLR9 expression vectors by the use of Lipofectamine 2000 (Life Technologies, Grand Island, N.Y.). pELAM-Luc (kindly provided by D. T. Golenbock) contains a human E-selectin promoter introduced into the pGL3 reporter plasmid (Promega, Inc., Madison, Wis.). The human TLR9 expression vector (kindly provided by T. H. Chuang) consists of a preprotrypsin signal peptide and a Flag epitope tag followed by an in-frame human TLR9 cDNA sequence (14). At 24 h posttransfection, the cells were stimulated with hCpG DNA (10 μg/ml) or AcNPV DNA (10 μg/ml) for 24 h. The luciferase activity was determined as previously described (49) and calculated as the degree of induction compared with an untreated control.

Detection of AcNPV capsid protein in murine macrophage cells by Western blot analysis. RAW264.7 murine macrophage cells (10^6 cells/well) infected with AcNPV at a dose of 40 μg/ml were washed extensively after 1 h of adsorption and harvested after 4 or 6 h of incubation. The cells were lysed in buffer containing 1% Triton X-100, 135 mM NaCl, 20 mM Tris-HCl (pH 7.5), 1% glycerol, and protease inhibitor cocktail tablets (Roche Molecular Biochemicals, Mannheim, Germany). The lysed sample was separated by SDS–12.5% PAGE and transferred to polyvinylidene difluoride membranes (Millipore, Tokyo, Japan). An anti-p39 mouse monoclonal antibody was used to detect the AcNPV capsid protein, which was visualized with the SuperSignal West Femto chemiluminescent substrate (Pierce).

RESULTS

Immune system activation by AcNPV is not mediated by viral envelope glycoprotein. It was previously reported that an IFN-stimulating preparation purified from Sf-9 cells infected with AcNPV exhibited IFN production both in vitro and in vivo
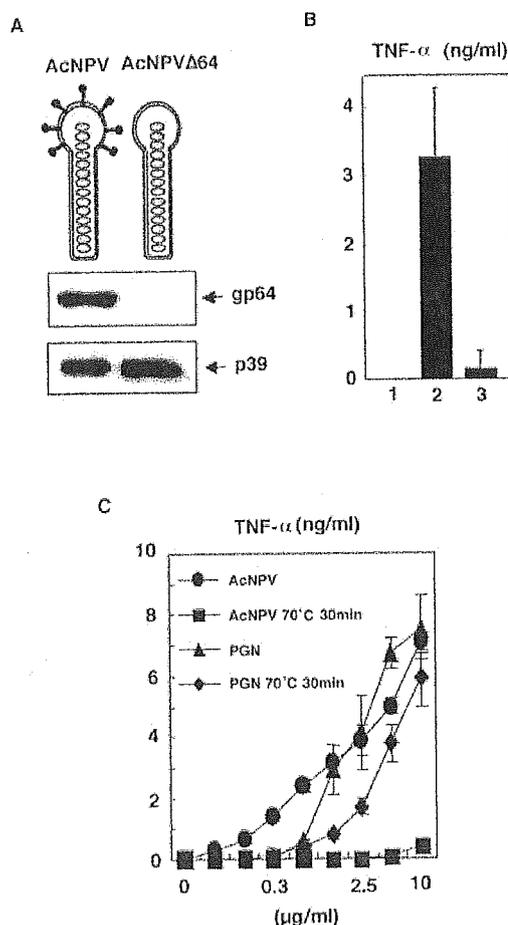

FIG. 1. Immune system activation of macrophages by heat-denatured or gp64-deficient AcNPV. (A) Purified particles of the mutant virus, AcNPVΔ64, lack gp64, as assayed by immunoblotting. (B) The production of TNF-α in RAW264.7 cells (10^6 cells/well) inoculated with AcNPV (5 μg/ml) (bar 2) or AcNPVΔ64 (5 μg/ml) (bar 3) was determined 24 h after inoculation by a sandwich ELISA. 1 is an uninfected control. Data are shown as means $\pm$ SD. (C) AcNPV and PGN were incubated at 70°C for 30 min. Treated and untreated samples were inoculated into RAW264.7 cells (10^6 cells/well) and incubated for 24 h. The production of TNF-α was determined by a sandwich ELISA. Data are shown as means $\pm$ SD.

and that induction was inhibited by monoclonal antibodies against the AcNPV envelope glycoprotein gp64 (18). To verify these observations, we constructed a mutant baculovirus lacking gp64, which we called AcNPVΔ64, and examined its ability to stimulate an immune response in RAW264.7 cells, which are highly sensitive to TLR stimulation and respond by producing inflammatory cytokines at a level comparable to that observed in primary macrophages (1). The absence of gp64 in purified particles of AcNPVΔ64 was confirmed by immunoblotting (Fig. 1A). The mutant virus lost the ability to induce TNF-α production in inoculated RAW264.7 cells (Fig. 1B), a result that is consistent with the previous observation that gp64 appears to play an important role in the induction of the immune response by AcNPV (18). Because some microbial products are known to induce cytokine production in macrophages, it was important to eliminate the possibility that contamination with microbial products contributed to the immune system

activation by AcNPV. Although the stimulation of macrophages by AcNPV was completely eliminated by incubation at 70°C for 30 min (Fig. 1C), stimulation by the bacterial components PGN and LPS was resistant to heat treatment (Fig. 1C and data not shown). These data indicate that the activation of macrophages by AcNPV is mediated by heat-labile viral components rather than by LPS and PGN.

To further verify the involvement of gp64 in immune system stimulation by baculovirus, we prepared expression plasmids encoding both wild-type gp64 and a C-terminally truncated gp64 protein (gp64ΔTM) with a C-terminal His$_6$ tag to allow for purification. Upon transfection of Sf9 cells, both recombinant proteins were detected, while gp64ΔTM was efficiently secreted into the culture supernatant (Fig. 2A). The protein from cells expressing gp64ΔTM was purified by column chromatography, producing a single band corresponding to gp64ΔTM and comparable to viral gp64 (Fig. 2B). We also tried to obtain the wild-type gp64 protein from the cell lysates but could not purify it to a homogeneous band (data not shown).

The activities of AcNPV, gp64ΔTM, and PGN on RAW264.7 cells were then examined. A dose-dependent induction of TNF-α and IL-6 was observed for RAW264.7 cells treated with AcNPV and PGN, whereas cytokine production was not observed for cells treated with gp64ΔTM (Fig. 2C). In addition, gp64ΔTM was not able to induce IFN-α production in RAW264.7 cells (Fig. 2D). Furthermore, the pretreatment of macrophage cells with gp64ΔTM inhibited immune system activation by AcNPV but had no effect on the activation by PGN (Fig. 2E), suggesting that the gp64ΔTM protein still retained some of the biological functions of the wild-type gp64 protein, at least in terms of its interaction with host cells. These results indicated that gp64 is an essential element of AcNPV-induced immune system activation in RAW264.7 cells but that it does not directly participate in the reaction. Viral components other than gp64 may be more directly involved in this process.

AcNPV induces inflammatory cytokine production through a MyD88/TLR9-dependent pathway. Immune cells from MyD88- or TLR-deficient mice are unresponsive to TLR ligands, as assayed by their levels of cytokine production (5). Therefore, we used PECs and splenic CD11c$^+$ DCs obtained from MyD88- and TLR-deficient mice to determine whether or not the TLR signaling pathway is responsible for the activation by AcNPV. Thioglycolate-elicited PECs were isolated from wild-type, MyD88$^{-/-}$, TLR2$^{-/-}$, TLR4$^{-/-}$, and TLR9$^{-/-}$ mice and examined by ELISA and Northern blot analysis for the induction of IL-12 following exposure to AcNPV. Wild-type macrophages inoculated with AcNPV produced large amounts of IL-12 in a dose-dependent manner, whereas MyD88- or TLR9-deficient macrophages had severely reduced IL-12 production (Fig. 3A). PECs from TLR2$^{-/-}$ and TLR4$^{-/-}$ mice produced IL-12 at wild-type levels in response to AcNPV (Fig. 3A).

Loxoribine is a potent inducer of cytokine production in macrophages and functions through a TLR7-dependent pathway (36). PECs from wild-type, TLR2$^{-/-}$, TLR4$^{-/-}$, and TLR9$^{-/-}$ mice all produced IL-12 in response to loxoribine, whereas no IL-12 production was observed in PECs from MyD88$^{-/-}$ mice (Fig. 3A). The transcription of IL-12 p40

mRNA was also impaired in MyD88- and TLR9-deficient macrophages stimulated with AcNPV (Fig. 3B). We further examined the response of splenic CD11c$^+$ DCs to AcNPV and loxoribine. Wild-type and TLR4$^{-/-}$ splenic CD11c$^+$ DCs produced IL-12 in response to AcNPV in a dose-dependent manner, whereas the production of IL-12 was severely impaired in MyD88$^{-/-}$ and TLR9$^{-/-}$ mice (Fig. 3C). In response to loxoribine, splenic CD11c$^+$ DCs from TLR4$^{-/-}$ and TLR9$^{-/-}$ mice exhibited higher IL-12 production levels than wild-type cells, whereas the production of IL-12 was completely inhibited in MyD88$^{-/-}$ mice (Fig. 3C). These results indicate that AcNPV induces the production of inflammatory cytokines in immunocompetent cells through a MyD88/TLR9-dependent pathway.

AcNPV produces IFN-α through a MyD88/TLR9-independent pathway. IFNs are important mediators of the early host defense against various viral infections. Since AcNPV has also been shown to be a potent inducer of IFN-α (Fig. 2D) (18), we investigated whether IFN-α production induced by AcNPV is dependent on the MyD88 and TLR9 signaling pathways. Although IFN-α induction by the TLR9 ligand, CpG oligonucleotides, was completely abolished in PECs and splenic CD11c$^+$ DCs derived from MyD88$^{-/-}$ or TLR9$^{-/-}$ mice (data not shown), IFN-α production in response to AcNPV was less impaired (Fig. 4A). This contrasted sharply with the complete loss of IL-12 production observed for these cells (Fig. 3). Macrophages from MyD88$^{-/-}$ and TLR9$^{-/-}$ mice exhibited a slight reduction in IFN-α and IFN-β mRNA transcription in response to AcNPV (Fig. 4B). These results indicate that AcNPV induces the production of inflammatory cytokines in immunocompetent cells through a MyD88/TLR9-dependent pathway, while other MyD88/TLR9-independent pathways are also involved in the production of IFNs.

AcNPV DNA stimulates immune system activation in macrophage cell lines. CpG motifs present in the genomes of many bacteria are unmethylated, whereas eukaryotic genomes are much more likely to undergo methylation. Previous work demonstrated that bacterial DNAs and certain oligonucleotides containing unmethylated CpG dinucleotides can stimulate PECs and DCs (19, 32). In addition, TLR9 is essential for the immune response to CpG-rich DNA, since TLR9-deficient mice are refractory to such stimulation (24). The frequency of bioactive CpG motifs in the AcNPV genome was similar to that observed for *Escherichia coli* and HSV DNAs (61) and significantly higher than that in murine and entomopoxvirus DNAs (Table 1).

To determine the methylation status of the AcNPV genome, we digested DNAs isolated from AcNPV, Sf-9 cells, *E. coli*, and 293T cells with the restriction enzyme HpaII, which cannot cleave when the cytosine adjacent to the cleavage site (CC↓GG) is methylated. While DNA isolated from 293T cells was refractory to HpaII digestion, DNAs from AcNPV, Sf-9 cells, and *E. coli* were sensitive to HpaII digestion, indicating that most of the CpG dinucleotides in AcNPV were unmethylated (Fig. 5A).

To determine the ability of AcNPV DNA to stimulate an immune response in vitro, we purified the viral DNA from virions. RAW264.7 cells were then treated with purified viral DNA or PGN with or without liposomes (Fig. 5B). The transfection of viral DNA with liposomes resulted in the production
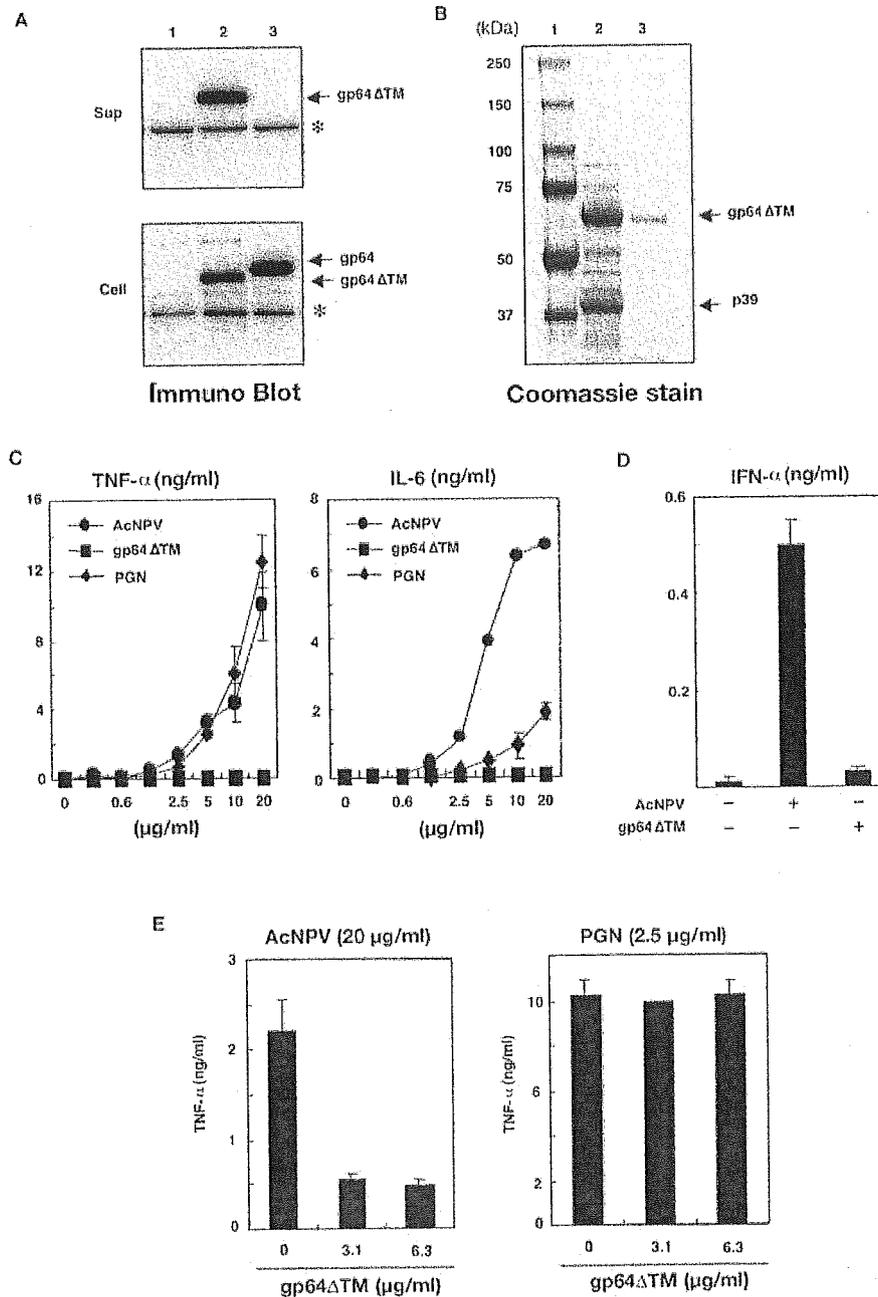
FIG. 2. Immune system activation by AcNPV in macrophages is not mediated by gp64. (A) Wild-type gp64 and a deletion mutant lacking the transmembrane region of the gp64 envelope protein (gp64ΔTM) were expressed in Sf-9 cells. Whole-cell lysates and culture supernatants were subjected to SDS-PAGE under reducing conditions and visualized by immunoblotting with an antihexahistidine monoclonal antibody. Lane 1, cells transfected with pIB/V5-His; lanes 2 and 3, cells transfected with pIBgp64ΔTM/V5-His and pIBgp64/V5-His, respectively. The heavy chains of the antibody are indicated by asterisks. (B) Purified AcNPV virions (lane 2) and gp64ΔTM (lane 3) were analyzed by SDS-PAGE and Coomassie blue staining. Lane 1, molecular mass markers. (C) Activation of mouse macrophage RAW264.7 cells (10^6 cells/well) treated with the indicated amounts of AcNPV or gp64ΔTM. The production of TNF-α and IL-6 in culture supernatants after 24 h of incubation was determined by sandwich ELISAs. PGN was used as a positive control. Data are shown as means ± SD. (D) Production of IFN-α in RAW264.7 cells (10^6 cells/well) inoculated with AcNPV (5 μg/ml) or gp64ΔTM (5 μg/ml), as determined by a sandwich ELISA after 24 h of incubation. Data are shown as means ± SD. (E) Production of TNF-α in RAW264.7 cells (10^6 cells/well) inoculated with AcNPV (20 μg/ml) or PGN (2.5 μg/ml), with or without a pretreatment with the indicated amounts of gp64ΔTM for 2 h at 37°C. After 24 h of incubation, the production of TNF-α in culture supernatants was determined by a sandwich ELISA. Data are shown as means ± SD.

of TNF-α, but this effect was not observed in the absence of liposomes. The enhancement of TNF-α production by liposomes was not observed in cells treated with PGN, and the addition of liposomes alone did not elicit TNF-α production

(Fig. 5C). These results indicate that the internalization of viral DNA is necessary for the activation of the AcNPV-mediated TLR9 signaling pathway. Thus, the impaired immune system activation by AcNPVΔ64 in macrophages may result from a
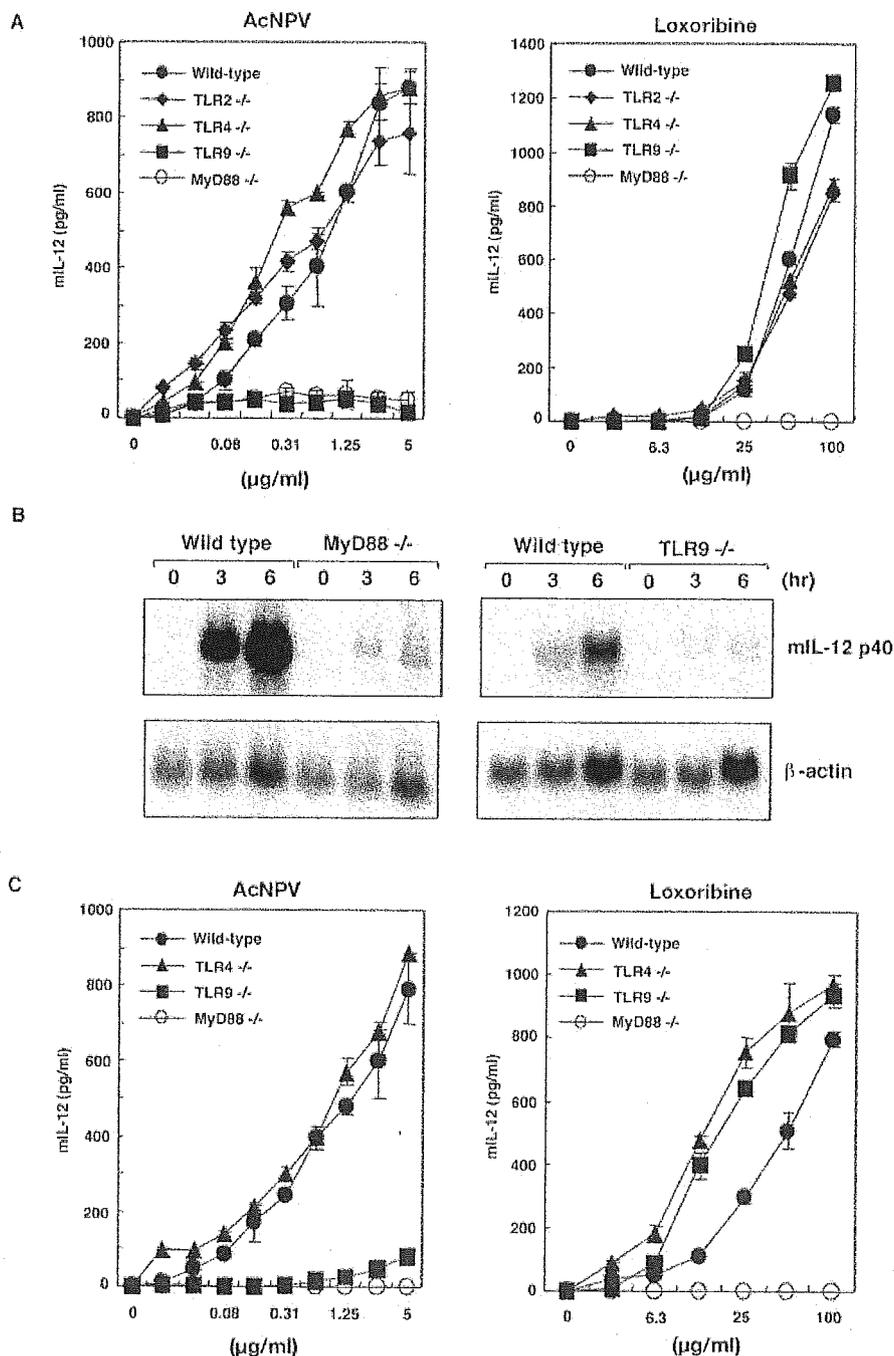
FIG. 3. AcNPV activates PECs and DCs in a MyD88/TLR9-dependent manner. (A) PECs (2 × 10⁵ cells/well) from wild-type (C57BL/6) or MyD88-, TLR2-, TLR4-, or TLR9-deficient mice were stimulated with the indicated amounts of AcNPV or loxoribine. The production of IL-12 p40 in culture supernatants was measured by a sandwich ELISA. Data are shown as means ± SD. (B) Northern blot analysis of murine macrophage cells stimulated with AcNPV. PECs (6 × 10⁶ cells/well) from wild-type or MyD88- or TLR9-deficient mice were stimulated with AcNPV (10 μg/ml) for the indicated times. Total RNAs were extracted and subjected to Northern blot analysis. (C) Splenic CD11c⁺ DCs were prepared from wild-type or MyD88-, TLR4-, or TLR9-deficient mice and enriched by magnetic cell sorting. Splenic DCs (10⁵ cells/well) were stimulated with the indicated amounts of AcNPV or loxoribine for 24 h. The production of IL-12 p40 in supernatants was measured by a sandwich ELISA. Data are shown as means ± SD.

failure to internalize viral DNA via gp64-mediated membrane fusion.

To further confirm that viral DNA activates the signaling pathway following internalization via gp64, we inactivated

AcNPV by UV irradiation and examined the production of TNF-α in RAW264.7 cells. UV irradiation diminished the AcNPV-mediated induction of TNF-α, but the addition of liposomes restored the activation (Fig. 5C). These results
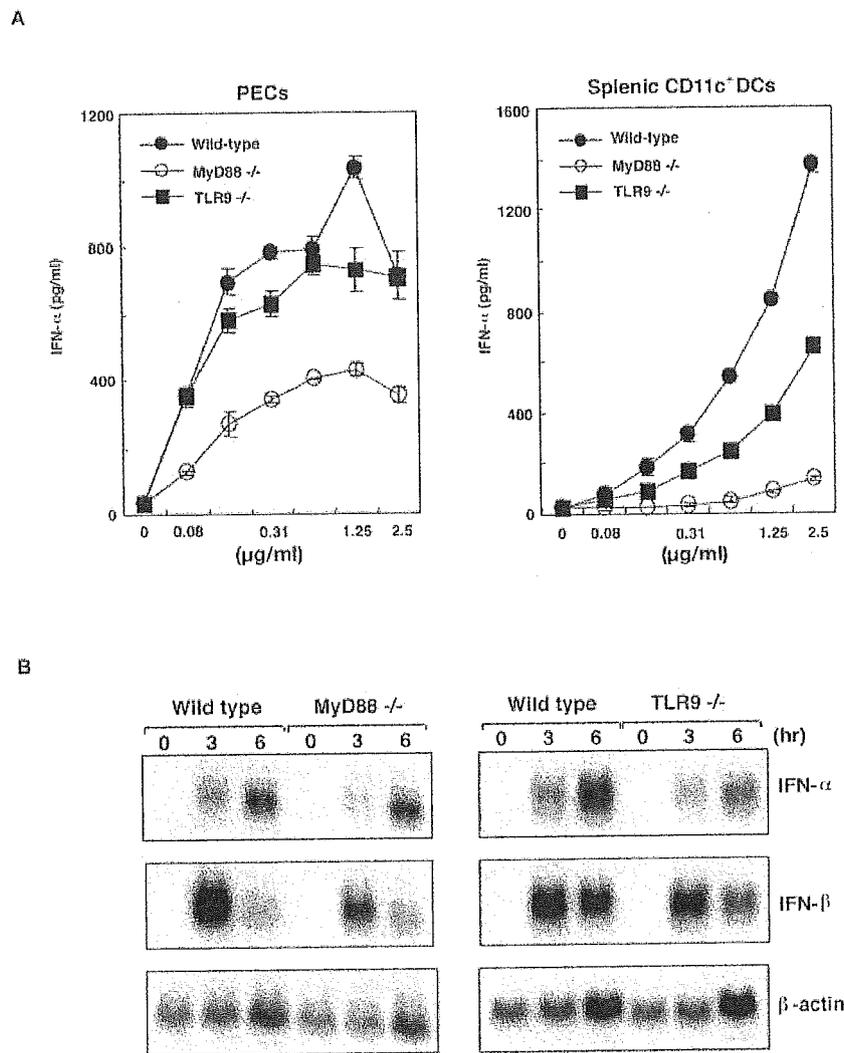
A

B

FIG. 4. IFN production by AcNPV is mediated by a MyD88/TLR9-independent process. (A) PECs (2 × 10⁵ cells/well) and splenic CD11c⁺ DCs (1 × 10⁵ cells/well) were prepared from wild-type or MyD88- or TLR9-deficient mice and stimulated with the indicated amounts of AcNPV or loxoribine for 24 h. The production of IFN-α in culture supernatants was measured by a sandwich ELISA. Data are shown as means ± SD. (B) Northern blot analysis of murine macrophage cells stimulated with AcNPV. PECs (6 × 10⁶ cells/well) from wild-type or MyD88- or TLR9-deficient mice were stimulated with AcNPV (10 μg/ml) for the indicated times. Total RNAs were then extracted and subjected to Northern blot analysis.

suggest that the denaturation of gp64 by UV irradiation impaired the fusion capability of the envelope protein, thus inhibiting the internalization of viral DNA into the cell via membrane fusion.

AcNPV DNA induces NF-κB activation through human TLR9. Signaling via TLRs occurs through the sequential recruitment of the adapter molecule MyD88 and the serine-threonine kinase IL-1 receptor-associated kinase, which leads to the activation of mitogen-activated protein kinases and the nuclear factor NF-κB (51). To assess whether or not the expression of human TLR9 confers cellular responsiveness to AcNPV DNA, we transfected 293T cells with a human TLR9 expression plasmid and a pELAM luciferase reporter plasmid together with AcNPV or hCpG, which was used as a positive control (Fig. 6A). Although NF-κB activation was not observed for cells transfected with undigested AcNPV DNA,

TABLE 1. CpG motif frequencies in AcNPV and other genomes[a]

Motif	Frequency of appearance				
	E. coli	Mouse	HSV-1	AcNPV	AmEPV
CACGTT	1.30	0.11	0.76	0.90	0.17
AGCGTT	1.70	0.17	0.42	1.12	0.15
AACGTC	0.60	0.11	0.73	0.98	0.17
AGCGTC	1.30	0.15	0.85	0.85	0.15
GGCGTC	1.40	0.15	4.0	1.10	0.02
GGCGTT	2.50	0.15	1.51	1.37	0.10
Average	1.53	0.14	1.38	1.05	0.13

[a] The frequency at which each CpG hexamer appeared in the E. coli, mouse, HSV-1, AcNPV, and Amsacta moorei entomopoxvirus genomes was determined by using published sequence data. The GenBank accession numbers for the complete genomes of AcNPV and AmEPV are NC 001623 and NC 002520, respectively. The complete genomes of E. coli K-12 and HSV-1 and mouse chromosome sequences were described previously (61).

A

B

C

A

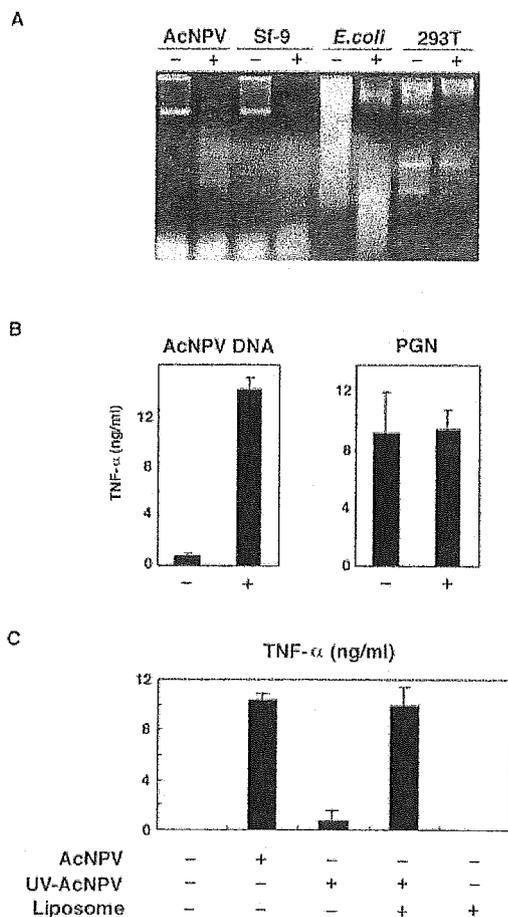|					
hTLR9 vector	+	+	+	−	−
Empty vector	−	−	−	+	+
Digested viral DNA	−	+	−	−	+
Undigested viral DNA	+	−	−	+	−
hCpG	−	−	+	−	−

B

C

FIG. 5. Activation of mouse macrophage cell line by AcNPV DNA. (A) Methylation status of genomic DNA. Genomic DNAs obtained from AcNPV, Sf-9 cells, *E. coli*, and 293T cells were digested with the methylation-sensitive restriction enzyme HpaII. Undigested (−) and digested (+) samples were analyzed by agarose gel electrophoresis. (B) RAW264.7 cells (10^6 cells/well) were treated with AcNPV DNA (5 μg/ml) or PGN (2.5 μg/ml) in the absence (−) or presence (+) of liposomes for 24 h, and the production of TNF-α in culture supernatants was determined by a sandwich ELISA. Data are shown as means ± SD. (C) Activation of RAW264.7 cells (10^6 cells/well) inoculated with untreated or UV-inactivated AcNPV (5 μg/ml) in the presence or absence of liposomes was assessed by the production of TNF-α in culture supernatants. Data are shown as means ± SD.

FIG. 6. AcNPV DNA induces NF-κB activation through human TLR9. (A) 293T cells were transfected with an empty or human TLR9 expression vector together with a pELAM luciferase reporter plasmid. Twenty-four hours after transfection, the cells were stimulated with digested or undigested AcNPV DNA (10 μg/ml). hCpG (10 μg/ml) was used as a positive control. The luciferase activity was determined at 24 h posttransfection and expressed as the level of induction compared with that detected in cells transfected with the human TLR9 expression vector alone. Data are shown as means ± SD. (B) Immunofluorescence micrographs of 293T cells transfected with an N-terminal Flag-tagged human TLR9 expression vector and stained with an anti-Flag (M2) monoclonal antibody. The intracellular (left) and cell surface (right) expression of TLR9 is shown. Nuclei were stained with propidium iodide (PI). Samples were observed by confocal microscopy. (C) The surface and intracellular expression of human TLR9 in 293T cells transfected with an N-terminal Flag-tagged human TLR9 expression vector (+) or an empty vector (−) and stained with an anti-Flag monoclonal antibody was examined by fluorescence-activated cell sorting.

HindIII-digested viral DNA and hCpG exhibited significant NF-κB activation, suggesting that undigested viral DNA is incapable of penetrating cells by transfection. No activation of NF-κB was observed in 293T cells cotransfected with a human TLR2 or TLR4 expression plasmid when stimulated with digested AcNPV DNA (data not shown).

Recent work demonstrated that the endogenous expression of TLR3, TLR7, TLR8, and TLR9 was mainly detected in the cytoplasmic vesicles of macrophages (58). To examine the localization of transiently expressed TLR9, we transfected 293T cells with a TLR9 expression plasmid and examined TLR9 expression by immunofluorescence microscopy and cell sorting. The expression of TLR9 in the cytoplasm was three times higher than that at the cell surface (Fig. 6B and C). These results indicate that the introduction of AcNPV DNA into the
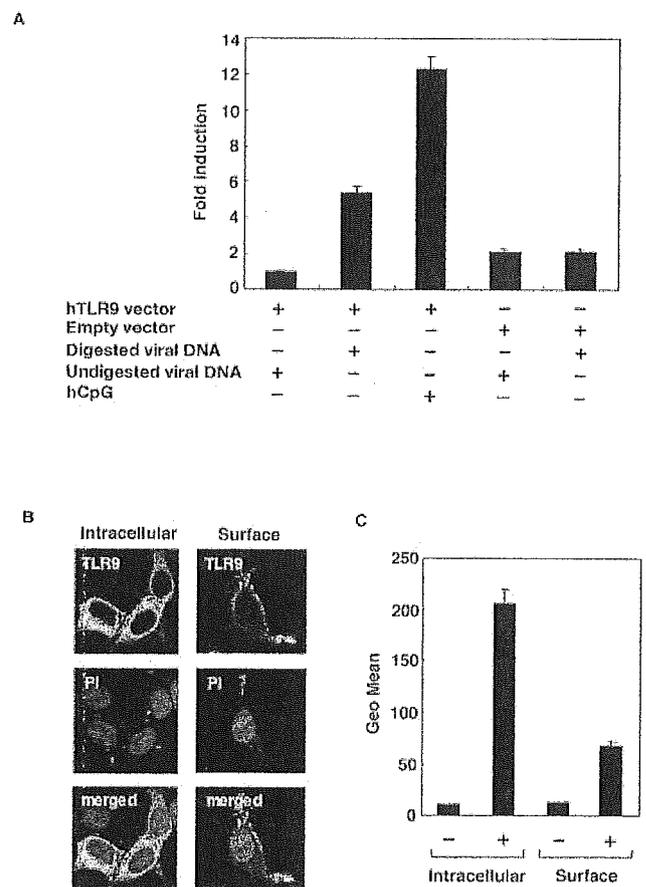
cytoplasm is specifically detected by human TLR9 and results in the activation of NF-κB.

AcNPV requires endosomal maturation to induce immune system activation in macrophages. To further explore the role of endocytosis in the signal transduction pathway triggered by AcNPV DNA, we examined the effect of endosomal maturation or acidification inhibitors. As shown in Fig. 7A, chloroquine was able to inhibit immune system activation of RAW264.7 cells treated with AcNPV and mCpG oligonucleotides in a dose-dependent manner, but no inhibition of LPS or PGN activation was observed. Other inhibitors of endoso-